

## Manuscript Details

<b>Manuscript number</b>	ATP_2017_147
<b>Title</b>	Solar proton events and stratospheric ozone depletion over northern Finland
<b>Article type</b>	Research Paper

### Abstract

We examine the variation of stratospheric ozone over northern Finland using ozonesonde observations from 1845 stratospheric balloon flights launched between 1989 and 2015 from near Sodankylä. The annual variation of the ozone partial pressure is examined and seasonal variations are explored and quantified. Direct links between the measured ozone partial pressure and common solar-wind parameters are also examined. A superposed-epoch analysis of the observations based on 191 solar proton events (SPEs) reveals a clear drop in the ozone partial pressure that commences following SPE-arrival at Earth. This analysis shows a reduction in stratospheric ozone in the winter/early-spring months (when the polar vortex is active over northern Finland), in contrast to summer/early-autumn months where no decrease is detected. By subtracting the natural seasonal variations in ozone partial pressure the SPE-driven reduction in ozone between 16 km and 24 km altitude is quantified. Analysis indicates that the ozone partial pressure during winter/early-spring is reduced, with a minimum reached ~8 days following the SPE arrival. On average, the ozone partial pressure is reduced by ~10% between 16-24 km altitude and takes ~40 days to return to its previous level. To the best of our knowledge, this is the first comprehensive statistical study, on a regional basis, that provides direct, and long-term in-situ evidence for ozone depletion by SPEs in the northern hemisphere.

<b>Keywords</b>	solar protons; ozone; space weather; energetic particle precipitation
<b>Manuscript category</b>	Stratosphere
<b>Corresponding Author</b>	Michael Denton
<b>Corresponding Author's Institution</b>	Space Science Institute
<b>Order of Authors</b>	Michael Denton, Rigel Kivi, Thomas Ulich, Craig Rodger, Mark Clilverd, Richard Horne, Andrew Kavanagh
<b>Suggested reviewers</b>	Jeffrey Thayer, Holger Vömel, Bryan Johnson, Martin Mlyneczek, Lauren Blum

## Submission Files Included in this PDF

### File Name [File Type]

response\_to\_reviewers\_denton.doc [Response to Reviewers]  
paper\_revised\_track\_changes.doc [Revised Manuscript with Changes Marked]  
highlights.doc [Highlights]  
paper\_revised.doc [Manuscript File]

## Submission Files Not Included in this PDF

### File Name [File Type]

fig01.png [Figure]  
fig02.png [Figure]  
fig03.png [Figure]  
fig04.png [Figure]  
fig05.png [Figure]  
fig06.png [Figure]

To view all the submission files, including those not included in the PDF, click on the manuscript title on your EVISE Homepage, then click 'Download zip file'.

**We thank both reviewers for their positive comments on our manuscript. The comments and suggestions have helped clarify our arguments and certainly resulted in an improvement to the manuscript.**

**We have addressed all comments below, with the changes detailed in the 'track changes' document that accompanies the revised submission.**

---

**Reviewer 1**

This paper presents results of investigating ozone loss in the stratosphere related to Solar Proton events and presenting the need to include energetic particle precipitation events (EPP) into climate models.

The northern latitude site in Sodanklyä in northern Finland was selected as the data source for analyzing mean monthly variation of stratospheric ozone plotted with various geophysical variables, and with a long record from 1989 to current of ozonesonde data (1,845 ozonesonde profiles). The details of the ozonesonde data used here are referenced in publication by Kivi et al. (2007) where several ozonesonde data sites were analyzed for stratospheric ozone loss correlating with stratospheric circulation, polar stratospheric clouds and effective equivalent stratospheric chlorine and include the QBO winds and solar cycle influence on ozone. They found 50% of the March ozone variability was due to springtime polar ozone depletion within the 50 hPa (~19 km) to 70 hPa (~17 km) altitude layer.

Another Arctic stratospheric ozone loss paper referenced is from Manney et al, (2011). The Manney paper discusses some of the well-known "ozone hole" ozone destruction processes (primarily over Antarctica) during the Arctic spring, especially in 2011. They attribute and correlate ozone loss with polar stratospheric clouds and chlorine catalytic chemistry that leads to ozone destruction which can be identified by decreasing HCl and increasing ClO which signifies chlorine activation. 2011 was a particularly low ozone episode for the Arctic spring time due to a stable vortex and very cold stratospheric temperatures. Manney et al. (2011) reported that chemical destruction was severe between 16 and 22 km. From ~18 to 20 km, more than 80% of the ozone present in January had been chemically destroyed by late March.

In contrast to the Kivi and Manney reports of high ozone loss in the stratosphere is the reference to Jackman et al, (1995b) on solar proton events on the middle atmosphere. Here they report that using models that NO<sub>x</sub> predicted lower-stratospheric polar ozone decreases of greater than 2% persisting for one and half years past the time when very large solar proton events had occurred in 1989.

The paper gives very good background and discussions, with numerous references, explaining the solar events and searching for trends by plotting ozone amount with 4 solar wind parameters especially searching for a link to direct destruction of stratospheric ozone by EPP:

Most papers on stratospheric ozone loss seem to be related to measurements and tracking and searching for recovery in the yearly ozone hole over Antarctica each spring. It has been interesting to learn more about solar proton events

and ozone through this paper and other references. My only 2 general questions are:

1. Do Arctic springtime chlorine-chemistry ozone depletion events affect the analysis when searching for trends related to solar wind parameters or EPP?

Note: this is mentioned in Line 254 with reference to Manney et al., (2011) when they reported severe ozone loss in 2011 from catalytic chlorine destruction under cold, stable vortex conditions when "ozone hole" type chemical destruction in Arctic regions was severe between 16 and 22 km. From ~18 to 20km, more than 80% of the ozone present in January had been chemically destroyed by late March.

**This is a key point. Arctic spring-time effects of chlorine-chemistry ozone depletion are certainly contained in the dataset. While it is difficult to extract these effects from the background analysis, we have tried to do this by subtracting off the seasonal means from the data. Simply removing data from 2011 (or other years) does not change the overall findings substantially.**

**An alternative approach is to compare sites that are inside and outside the polar vortex in springtime and we are currently working on a follow-up study that considers just this issue, using a variety of different ozonesonde stations (in and out of the vortex). We will hopefully be able to answer this question more fully in the near future. In the meantime we have added some text in Section 3.1 and Section 5 to clarify this point specifically.**

2. Is the ozonesonde data (one flight per week from surface to 32 km) sufficient for analysis? Would satellite data provide better data, especially at higher altitudes?

This is briefly mentioned in line 348.

**Yes, more data would always be welcome. The data from Finland are certainly extensive as far as long-term balloon data go. Balloon data have the advantage of providing altitude profiles (and the altitude variation) of the ozone, rather than just column-averages that are typical of satellite data. And we actually have more than once-per-week data as there are campaign data in many years where daily ozonesondes are flown for up to 10 consecutive days (line 69-72). However, it would indeed be very good to see this study repeated with global satellite column-integrated ozone data. We have clarified this point in Section 2 and also included some extra text in the Summary section - we would certainly welcome collaboration on repeating/extending this study with satellite data.**

Line 64: It would be helpful to see the altitude given in km (30-34 km) along with lower stratosphere - "These instruments are capable of providing profile measurements of ozone concentrations from the surface to the lower stratosphere (30-34 km)."

**Agreed. Changed as suggested.**

Line 205: The sentence: "Though the plots show the average (mean) ozone partial pressure up to 40 km altitude (top row)." It would be unlikely a balloonborne ozonesonde will reach 40 km altitude. Typical maximum altitudes are around 30-32 km. 38 km is rare but possible.

**Agreed. We have clarified as suggested.**

Line 605 Figure 3: "The" change to "There"

**Changed as suggested.**

**Reviewer 2**

The paper by Denton et al. "Solar proton events and stratospheric ozone depletion over northern Finland" is a comprehensive study which convincingly shows the correlation between ozone depletion and solar proton events. Statistical analysis of balloon measurements near Sodankyla from 1989 to 2015 shows average 10% reduction in stratospheric ozone partial pressure in connection with SPE events. I have several comments and suggestions to the paper:

1. Introduction, lines 38-38: Odd nitrogen is not the only intermediate cause for stratospheric ozone depletion. Chlorine species are also important contributors in the upper stratosphere, e.g.,

Jackman, C. H., D. R. Marsh, F. M. Vitt, R. R. Garcia, C. E. Randall, E. L. Fleming, and S. M. Frith (2009), Long-term middle atmospheric influence of very large solar proton events, *J. Geophys. Res.*, 114, D11304, doi:10.1029/2008JD011415.

Damiani, A., M. Storini, M. Laurenza, and C. Rafanelli (2008), Solar particle effects on minor components of the polar atmosphere, *Ann. Geophys.*, 26, 361-370.

Damiani, A., P. Diego, M. Laurenza, M. Storini and C. Rafanelli (2009), Ozone variability related to several SEP events occurring during solar cycle no. 23, *Adv. Space Res.*, 43, 28-40.

Damiani, A., et al. (2012), Impact of January 2005 solar proton events on chlorine species, *Atmos. Chem. Phys.*, 12, 4159-4179.

**Good point. We have clarified the text and included the references suggested, although in detail in Section 3, rather than Section 1.**

2. Lines 47-49: it might be relevant to mention a comprehensive recent study on atmospheric ionization chemistry:

Verronen, P. T., and R. Lehmann (2013), Analysis and parameterisation of ionic reactions affecting middle atmospheric HOx and NOy during solar proton events, *Ann. Geophys.*, 31, 909-956, doi:10.5194/angeo-31-909-2013.

**Agreed. We have now included this reference.**

3. Line 91: please, provide your definition of geopotential altitude (height). Typically pressure units are used instead of altitude in km.

**As is common for ground-based data, we typically use geopotential height for easier comparison with other ground-based measurements (e.g. lidar). The full definition can be found at**

[www.mathpages.com/home/kmath054/kmath054.htm](http://www.mathpages.com/home/kmath054/kmath054.htm)

or in brief at

[glossary.ametsoc.org/wiki/Geopotential\\_height](http://glossary.ametsoc.org/wiki/Geopotential_height)

**but this derivation would be a bit too much of a sidetrack for inclusion here. We have included some summary text in the paper.**

4. Lines 137-159: Because of the large number of data points, it might be instructive to plot Figure 3 but for the Jan-April selection when the ozone is higher as seen in Figure 1. I can not understand the lack of correlation with F10.7 index. Maybe this is the question of how to represent/plot the data and possible overlapping of data points. Maybe a cumulative diagram can be helpful.

**We did try a bunch of different types of plot for these data to try and show the correlation with F10.7 (which we also expected initially). It appears that the daily/monthly seasonal variations are generally greater than the long term F10.7 variation. You can see this by comparison with Figure 2. The years with high F10.7 (around solar max) do show up, but there is no very clear and consistent variation with F10.7. We comment on this on lines 101-102.**

5. Lines 257-267: Precipitating high-energy electrons can also cause NOx increase:

Randall, C. E., V. L. Harvey, L. A. Holt, D. R. Marsh, D. E. Kinnison, B. Funk and P. F. Bernath (2015), Simulation of energetic particle precipitation effects during the 2003-2004 Arctic winter, *Journal of Geophysical Research : Space Physics*, 120, 5035-5048, doi:10.1002/2015JA021196.

Thus, magnetospheric electron precipitation (in a high energy end of the spectrum) can be another factor. Strong SPEs are often associated with CMEs and SPEs timings can be close to occurrences of CME-type storms. However, magnetospheric electron acceleration and precipitation can be delayed into a storm recovery phase, e.g., peak electron precipitation will not coincide in time with a SPE.

**Agreed. This is something we've very familiar with and have explored in detail. Looking for long-term and short-term effects due to electrons in a variety of different types of event actually kickstarted this entire study. However, many of the SPEs studied here are not associated with storms (CME-storms or other types). We do not expect electron precipitation from the radiation belts to be significant (on average) for these events. We have included some additional text and the suggested reference as requested.**

6. Line 292-293: You could note here that studies of particle precipitation effects on mesosphere and upper stratosphere have been an active area of research since around 80s (see the references below). However, the lower stratospheric effects have not received as much attention until modeling by Randall et al. on indirect effects of EPP. I am not sure this effect is under-appreciated now.

Rusch, D. W., J.-C. Gérard, S. Solomon, P. J. Crutzen, and G. C. Reid (1981), The effect of particle precipitation events on the neutral and ion chemistry of the middle atmosphere: I. Odd nitrogen, *Planet. Space Sci.*, 29(7), 767.

Solomon, S., D. W. Rusch, J.-C. Gérard, G. C. Reid, and P. J. Crutzen (1981), The effect of particle precipitation events on the neutral and ion chemistry of the middle atmosphere: II. Odd hydrogen, *Planet. Space Sci.*, 29(8), 885-893.

Solomon, S., D. W. Rusch, R. J. Thomas, and R. S. Eckman (1983), Comparison of mesospheric ozone abundance measured by the Solar Mesosphere Explorer and model calculations, *Geophys. Res. Lett.*, 10, 249-252, doi:10.1029/GL010i004p00249.

**Noted as suggested. We have reordered the text and these additional references are also included.**

# Solar proton events and stratospheric ozone depletion over northern

## Finland

*M. H. Denton<sup>1,2</sup>, R. Kivi<sup>3</sup>, T. Ulich<sup>4</sup>, C. J. Rodger<sup>5</sup>, M. A. Clilverd<sup>6</sup>, R. B. Horne<sup>6</sup>, A. J. Kavanagh<sup>6</sup>.*

1. Space Science Institute, Boulder, CO 80301, USA.

2. New Mexico Consortium, Los Alamos, NM 87544, USA.

3. Arctic Research Centre, Finnish Meteorological Institute, Sodankylä, Finland.

4. Sodankylä, Geophysical Observatory, Sodankylä, Finland.

5. Department of Physics, University of Otago, New Zealand.

6. British Antarctic Survey ([NERC](#)), Cambridge, UK.

### ABSTRACT:

We examine the variation of stratospheric ozone over northern Finland using ozonesonde observations from 1845 stratospheric balloon flights launched between 1989 and 2015 from near Sodankylä. The annual variation of the ozone partial pressure is examined and seasonal variations are explored and quantified. Direct links between the measured ozone partial pressure and common solar-wind parameters are also examined. A superposed-epoch analysis of the observations based on 191 solar proton events (SPEs) reveals a clear drop in the ozone partial pressure that commences following SPE-arrival at Earth. This analysis shows a reduction in stratospheric ozone in the winter/early-spring months (when the polar vortex is active over northern Finland), in contrast to summer/early-autumn months where no decrease is detected. By subtracting the natural seasonal variations in ozone partial pressure the SPE-driven reduction in ozone between 16 km and 24 km altitude is quantified. Analysis indicates that the ozone partial pressure during winter/early-spring is reduced, with a minimum reached ~8 days following the SPE arrival. On average, the ozone partial pressure is reduced by ~10% between 16-24 km altitude and takes ~40 days to return to its previous level. To the best of our knowledge, this is the first comprehensive statistical study, on a regional basis, that provides direct, and long-term in-situ evidence for ozone depletion by SPEs in the northern hemisphere.

CORRESPONDING AUTHOR: M. H. Denton ([mdenton@spacescience.org](mailto:mdenton@spacescience.org))

## 31 1. Introduction

32 Solar proton events (SPEs) arise in association with energetic events on the Sun and energisation processes in  
33 interplanetary space (e.g. *Reames [1999]; Kurt et al. [2004], Tylka et al. [2006], Oh et al., [2010]*, and  
34 references therein). Upon arrival at Earth the solar protons may enter the upper atmosphere and collide with  
35 neutral particles at altitudes that are dependent on the incident energy of the protons [*Seppälä et al., 2008*]. At  
36 this point they induce chemical changes to the local neutral population. Such energetic particle precipitation  
37 (EPP) is regularly implicated in the production of species such as odd nitrogen ( $\text{NO}_x$ ) (e.g. *Crutzen et al. [1975];*  
38 *Shumilov et al. [2003]; Clilverd et al. [2005]*), which are themselves implicated in the subsequent depletion of  
39 stratospheric ozone. Odd-nitrogen species are long-lived during darkness and can descend to stratospheric  
40 altitudes via the high-latitude polar vortex, during the polar winter. Once at stratospheric altitudes  $\text{NO}_x$  may  
41 cause chemical destruction of the in-situ ozone (e.g. *Jackman et al. [1995]; Jackman et al. [2009]*). Other  
42 chemical pathways for ozone destruction are also available (e.g. *Jackman et al. [2009]; Damiani et al. [2008,*  
43 *2009, 2012]*). Observational case studies of large individual SPEs reveal that such ozone depletions (in the  
44 mesosphere and stratosphere) do indeed occur (e.g. *Weeks et al. [1972]; Heath et al. [1977]; Thomas et al.*  
45 *[1983]; López-Puertas et al. [2005]; Seppälä et al. [2004; 2006; 2008]*). Modelling studies of such events have  
46 also helped ascertain the long and short term implications for atmospheric ozone balance (e.g. *Jackman and*  
47 *McPeters [1985]; Jackman et al. [1996]; Rodger et al. [2008]; Jackman et al. [2009]*). More general **studies**  
48 recent studies of the effects of EPP have outlined some of the chemical changes that occur during SPEs (e.g.  
49 *Verronen and Lehman [2013]*) and also recently drawn links between geomagnetic activity, particle  
50 precipitation, and changes in polar surface air temperature [*Seppälä et al., 2009*]. However, a complete  
51 understanding-accounting of the chemical changes in the atmosphere resulting from EPP, and their relative  
52 importance, remains a major unsolved issue in magnetospheric and atmospheric physics [*Denton et al., 2016*].

53  
54 In the current study we aim to expand upon current knowledge by using a large database of ozone measurements  
55 constructed from 1845 *ozonesonde* balloon flights, launched from Sodankylä in northern Finland, between 1989  
56 and 2015 [*Kivi et al., 2007*]. Initially, these data are analysed to examine the seasonal/annual changes that occur  
57 in the ozone partial pressure in this region. Following this, links between the stratospheric ozone partial  
58 pressure and various common solar-wind parameters are explored. Subsequently, we carry out a statistical  
59 analysis of SPE-induced changes in stratospheric ozone during 191 SPE events that took place over the same  
60 time period as the ozonesonde observations. Finally, we quantify the observed reductions measured in the

61 ozone partial pressure following SPEs and discuss the implications of our findings, in comparison with other  
62 reported observations.

63

## 64 **2. Ozonesonde Data Set**

65 The ozone profiles used in this study were obtained by the electrochemical concentration cell (ECC) type of  
66 ozonesonde [Deshler *et al.*, 2008; 2017, Kivi *et al.*, 2007, Smit and ASOPOS Panel, 2014]. These instruments  
67 are capable of providing profile measurements of ozone concentration from the surface to the lower stratosphere  
68 (~30-34 km) with precision better than 2-3 % [Deshler *et al.*, 2008]. Vertical resolution of the soundings is  
69 about 10 meters, as data is typically analyzed in 2 second intervals, while the effective vertical resolution is of  
70 the order of 100-150 meters, given that the sensor response time is 20-30 seconds. The sondes used in this study  
71 have been launched on a regular basis from Sodankylä, Finland (67.4 N, 26.6 E) since 1989 during all seasons.  
72 Sondes are normally launched once per week around local noon. These data are supplemented by the frequent  
73 ozonesonde campaigns that have taken place in winter/spring season, significantly increasing the number of  
74 launches and the available dataset. This measurement program has resulted in 1845 soundings over the 27-year  
75 time period studied here. Balloon ozonesonde data have the advantage over satellite data that they provide high  
76 spatial resolution altitude profiles of the ozone distribution throughout the lower stratosphere. However, while  
77 these data are certainly suitable for study of changes in the ozone distribution over northern Finland, it should be  
78 noted that results will only apply on a local/regional basis. The details of the ozonesonde sounding system and  
79 principles of the data set homogenization are explained in detail in Kivi *et al.* [2007].

80

81

82

## 83 **3. Analysis and Results**

84

### 85 **3.1 Seasonal and Annual Variations of Stratospheric Ozone**

86

87 As previously shown by Kivi *et al.* [2007], there is a substantial annual variation in the stratospheric ozone  
88 partial pressure over Sodankylä during the year with a peak ozone level occurring around April and a minimum  
89 occurring around September (see Kivi *et al.* [2007], Figure 4). The annual cycle of ozone in the Arctic lower  
90 stratosphere is caused by the global annual cycle in ozone transport from lower latitudes towards the poles (e.g.

91 *Butchart*, [2014], and references therein). This transport is strongest in winter and early spring and the ozone  
92 variability is highest during this period. The stratospheric ozone concentrations in late spring and summer  
93 decrease continuously at high latitudes since the combination of ozone production and transport are too slow to  
94 offset the destruction of ozone via reactions involving  $\text{NO}_x$ . Significant destruction of ozone also occurs during  
95 via catalytic reactions involving chlorine monoxide (ClO) and bromine monoxide (BrO), but only during  
96 periods of sunlight (i.e. not during the polar winter) (e.g. *Jackman et al.* [2009]; *Damiani et al.* [2008, 2009,  
97 2012]). —To take account of the annual and seasonal variability of ozone in our analysis, we initially  
98 extend the analysis of *Kivi et al.* [2007], who calculated the average monthly variation of stratospheric ozone  
99 between 1989 and 2003. Here, this calculation is extended, using a further twelve years of data to cover the  
100 years 1989 to 2015 inclusive (cf. Section 3.3).

101

102 The average ozone partial pressure (in mPa) is calculated as a function of geopotential altitude (in km) and  
103 month of the year, for the entire ozonesonde dataset between 1989 and 2015.—The results of this analysis are  
104 shown in Figure 1. (Note: As is common with sonde data we use geopotential altitude (height) rather than  
105 pressure -units on the y-axis - the geopotential altitude approximates the altitude above sea-level of a particular  
106 pressure level). Clearly there is significant variability in the measured ozone on an inter-annual basis, which is  
107 largely due to inter-annual variability in chemical and dynamical factors influencing ozone. This inter-annual  
108 variability is strongly pronounced in the northern hemisphere, where dynamical variability is relatively large  
109 from year to year in contrast to the Antarctic stratosphere. However, significant vortex ozone depletions have  
110 also been observed in the northern hemisphere [*Manney et al.*, 2011].

111

112 To explore the annual variations in the ozone data we examine the entire dataset of balloon-borne ozonesonde  
113 measurements made above northern Finland between 1989 and 2015, plotted in Figure 2 (top panel). It is clear  
114 that the regular seasonal variations (cf. Figure 1) are a prominent feature in this dataset, but there are also large  
115 changes on a year-to-year basis. For example, the measurements around 2001, close to solar maximum, are  
116 noticeably higher than most other periods.

117

118 To quantify these changes we also plot these data on a seasonally-adjusted *difference-from-mean* basis (Figure  
119 2, bottom panel). The mean ozone partial pressure for the appropriate month and altitude (i.e. from the data  
120 shown in Figure 1) is subtracted from each individual measured ozone point in the data set. Doing this should

121 remove seasonal trends from the data and allow variations due to other causes to be detected. The *resulting*  
122 seasonally-adjusted difference-from-mean parameter plotted in Figure 2 ~~thus~~ provides quantification of the  
123 strength of the ~~annual~~-variations on an annual basis. For example, for the data around 2001, the measured ozone  
124 is at times ~8 mPa higher than the mean value (at around 20 km altitude). In contrast, the measured ozone  
125 partial pressure is at times ~8 mPa lower than its mean value in 1993 (at around 15 km altitude). The years  
126 around solar maximum (when the solar EUV flux and F10.7 index are higher) show evidence of generally  
127 higher ozone levels compared to the years around solar minimum(when the solar EUV flux and F10.7 index are  
128 lower). ~~However,~~although this certainly isn't always true in every year with elevated F10.7 and there is much  
129 variation. The causes of annual variations are also known to include: (i) "internal" terrestrial effects such as the  
130 quasi-biennial oscillation (QBO) cycle and volcanic eruptions that perturb aerosol concentrations, etc., (ii)  
131 longer-term "external" effects such as the 11-year solar cycle, and (iii) longer-term internal trends in  
132 stratospheric ozone as a result of anthropogenic causes [Kivi *et al.*, 2007; Manney *et al.*, 2011]. A more  
133 comprehensive discussion of the annual cycle, inter-annual variability and also day-to-day variability of  
134 stratospheric ozone over Sodankylä may be found in Kivi *et al.* [2007].

### 136 3.2 Variations of Stratospheric Ozone with Solar and Geophysical Parameters

137  
138 The literature contains various modelling and case-study results that show links between the state of the  
139 incoming solar wind, the subsequent state of the magnetosphere, and the terrestrial ozone population, in  
140 particular ozone in the mesosphere and ozone in the stratosphere. Considering the stratosphere, two physical  
141 mechanisms have been suggested that are thought to cause changes in the ozone population based on solar-wind  
142 driving; (i) instantaneous destruction of O<sub>3</sub> due to EPP by extremely energetic incident protons (with energies  
143 greater than ~100 MeV), whereby these penetrate the atmosphere directly to near-stratospheric altitudes and  
144 cause immediate ozone dissociation, and (ii) a longer time-scale process whereby odd-nitrogen species, for  
145 example, are created at mesospheric altitudes (by lower-energy particle precipitation due to both electrons or  
146 protons) and these then descend to stratospheric altitudes during the polar winter. At stratospheric altitudes  
147 these species cause chemical destruction of ozone. The latter process is often termed in the indirect effect, and  
148 the former the direct effect. Initially, we aim to test the efficacy of the direct effect by exploring links between  
149 solar-wind/geophysical parameters with the stratospheric ozone partial pressure. To investigate near-  
150 instantaneous changes in the ozone population we aim to correlate between the measured ozone partial pressure

151 and the level of various geophysical parameters measured 24 hours previously.

152

153 Figure 3 contains plots of the ozonesonde observations as a function of altitude, and four geophysical and solar-  
154 wind parameters, namely: (i) The Auroral Electrojet (AE) index, a commonly used parameter that is a good  
155 proxy for magnetospheric substorm activity [Davis and Sugiura, 1966; Gjerloev et al., 2004], (ii) the solar-wind  
156 electric field parameter ( $-v_{sw}B_z$ ) calculated as the negative product of the solar-wind velocity ( $v_{sw}$ ) and the z-  
157 component of the solar-wind magnetic field ( $B_z$ ), and measured in units of  $\text{mV m}^{-1}$ , (iii) the adjusted F10.7  
158 index, a measure of the incident radio flux at 10.7 cm, and a good proxy for ionising solar EUV radiation  
159 [Tapping, 2013, and references therein], and (iv) the Disturbance Storm Time (Dst) index [Sugiura, 1964;  
160 Skopke, 1966], a widely used measure of magnetospheric storm strength and a proxy for the strength of the  
161 Earth's ring current, measured in units of nT. All parameters used are taken from the hourly OMNI2 database  
162 [King and Papitashvili, 2005]. The aim of this analysis is to search for trends showing near-instantaneous  
163 changes in the ozone population as a result of changes driven by external solar wind parameters. If present,  
164 such changes could then be linked to direct destruction of stratospheric ozone by energetic particle precipitation.

165

166 It is clear from the plots shown in Figure 3 that there is little evidence for such changes on a systematic basis.  
167 None of the plots show clear trends in the ozone partial pressure as a result of increases or decreases in the  
168 parameters examined. Perhaps the most surprising result here is that there is no clear correlation with the F10.7  
169 index since stratospheric ozone is known to be correlated with solar irradiance [Kivi et al., 2008]. In Figure 1  
170 the highest ozone levels (above the mean) come in years around solar maximum although this isn't by any  
171 means a hard and fast rule. For example, in 2006 near solar minimum, the average ozone levels were above  
172 average even though the F10.7 index during the year rarely exceeded 100. It is known that other physical  
173 variables also strongly affect the annual transport and destruction of stratospheric ozone during each year and  
174 that these can certainly suppress variations based on the UV variation alone (see for example Kivi et al. [2007]  
175 and Manney et al. 2011]).

176

177 Whilst the literature does contain example case-studies of some of the largest geomagnetic storms resulting in  
178 rapid decreases in stratospheric ozone, it is also known that many of these 'extreme' events contain multiple  
179 drivers of geomagnetic activity such that no single index currently accounts for all causes of driving. The  
180 results from Figure 3 provide evidence that using fluctuations in a single geophysical index alone are not

181 sufficient to use as a predictor of subsequent changes in the near-instantaneous ozone partial pressure in the  
182 stratosphere. If such changes are occurring, a more sophisticated analysis to reveal them is required.

183

### 184 **3.3 The Effects of Solar-Proton Events (SPEs) on Stratospheric Ozone**

185

186 In order to explore changes in stratospheric ozone, beyond the systematic seasonal variations shown in Figure 1,  
187 and the annual variations shown in Figure 2, we examine external driving of the atmosphere by solar-proton  
188 events. Many studies of non-terrestrial drivers of changes in the ozone population focus on such events, since  
189 the particle spectrum is sufficiently hard that the most energetic particles can penetrate deep into the  
190 mesosphere, into the stratosphere, and even to ground level (e.g. *Solomon et al.* [1981], *Thomas et al.* [1983],  
191 *Jackman and McPeters.* [1985], *Clilverd et al.* [2005], *Verronen et al.* [2011] *Damiani et al.* [2016], *Hocke*  
192 [2017]). For the most energetic solar-terrestrial event yet known in the modern era, the 1859 Carrington Event,  
193 it has even proved possible to model the effects of extremely high fluxes of solar protons on the ozone balance  
194 within the atmosphere [*Rodger et al.*, 2008]. However, in contrast to event studies of very large events, or  
195 theoretical studies of long-term trends, it has proven difficult to make estimates of the long-term effects of more  
196 frequent, but less extreme, events particularly on a regional level. A recent study by *Damiani et al.* [2016] has  
197 addressed this issue, in part, for the southern hemisphere by showing a 10-15% decrease in stratospheric ozone  
198 over Antarctica using limb-sounding methods from the Aura satellite. That study found that descent of  
199 mesospheric NO<sub>x</sub> down to stratospheric heights was the primary cause of such stratospheric ozone depletion in  
200 the southern hemisphere. The authors also highlighted the limited observational evidence available to quantify  
201 particle precipitation effects upon the ozone budget in general [*Damiani et al.*, 2016]. Here, we attempt to  
202 address this issue for the northern hemisphere.

203

204 As a basis for the analysis we utilize a list of 191 Solar Proton Events taken from the published list by the US  
205 National Oceanic and Atmospheric Administration (NOAA) Space Weather Prediction Center (SWPC) and  
206 freely available via file transfer protocol (<ftp://ftp.swpc.noaa.gov/pub/indices/SPE.txt>). At the time of the  
207 analysis, only one SPE event was listed beyond the end of 2015. The epoch times taken from the NOAA list are  
208 the start-times of each individual SPE, at a time resolution of one-hour.

209

210 Analysis is then carried out by performing a superposed epoch study of the measured ozone during these events.

211 All available ozonesonde data are binned as a function of epoch time (time from SPE-onset) and geopotential  
212 altitude. The final grid for this binning is one day in time and 1 km in geopotential altitude, and spans a total of  
213 90 days: 30 days prior to the SPE through to 60 days after the SPE. In addition, a set of 2500 randomly selected  
214 epochs between 1989 and 2015 are generated using the methodology of *Park and Miller* [1988]. The ozone data  
215 are then sorted based on these random epochs with this analysis providing a control data set against which the  
216 SPE analysis can be compared. Note that no account is made of short-term diurnal effects.

217  
218 Figure 4 contains a selection of plots resulting from this analysis and shows the ozone partial pressure as a  
219 function of geopotential altitude and epoch time for (a) 2500 random epochs selected between 1989 and 2015  
220 (left column), and (b) 191 solar proton events that occurred during the same interval (right column). The plots  
221 show the averaged (mean) ozone partial pressure up to 40 km altitude (top row). No adjustment is made for  
222 seasonal variations in the data at this point. Also shown are line plots of the integral of the ozone partial  
223 pressure for altitudes between 16 and 24 km (middle row) for these events. This altitude region contains the  
224 bulk of stratospheric ozone (cf. Figure 1). The red points represent the individual data (i.e. the mean ozone  
225 partial pressure) and the blue line is a 15-day running box-car average of these data. (Note: the reduction in the  
226 running mean commences slightly prior to zero-epoch due to the 15-day averaging, although the individual (red)  
227 data points indicate ozone remains high until SPE arrival). The grey shading indicates the standard deviation of  
228 the superposition, whilst the thin orange, black, and purple lines represent the upper quartile, the median, and  
229 the lower quartile of the superposition.

230  
231 The plots in the top two rows of Figure 4, although suggestive of a decrease in total stratospheric ozone  
232 following SPE occurrence, take no account of the large seasonal variations in the ozone partial pressure known  
233 to exist over Sodankylä. In order to remove the seasonal variations in the data contributing to the superposed  
234 epoch analysis the mean ozone partial pressure for the month in question (taken from the values in Figure 1) is  
235 subtracted from each data point. The resulting quantity is thus seasonally independent. The bottom row in  
236 Figure 4 shows the summation of these 'difference-from-mean' values. Here, a negative value indicates a  
237 seasonally independent (i.e. a true) reduction in ozone partial pressure. As can be seen from Figure 4, there are  
238 only small fluctuations in the ozone partial pressure in all three plots for the random epochs. However, for the  
239 SPEs there is clear evidence for a decrease in the ozone partial pressure that commences close to the zero epoch  
240 and reaches a minimum value after around 8 days. This is evident especially in the line plots showing the

241 summed ozone partial pressure Here, the decrease in the ozone partial pressure (summed between 16-24 km) is  
242 of the order of 5%. The seasonally adjusted ozone partial pressure immediately prior to the zero epoch is  
243 slightly above the mean value but then falls rapidly around zero epoch, reaching a minimum after around 8 days,  
244 and then remains below the seasonally adjusted mean value for around 40 days.

245

246 While it is unlikely that protons with energies lower than ~10-100 MeV will directly reach the atmosphere  
247 above Sodankylä due to geomagnetic field rigidity effects (see *Rodger et al.* [2008], Figure 8), these protons  
248 will produce NO<sub>x</sub> at higher latitudes. This is then likely to be rapidly mixed throughout the polar vortex, and  
249 thus may contribute to indirect, time-delayed ozone depletion, particularly when the polar vortex extends to the  
250 Sodankylä region. This occurs around 50% of the time between December and April and never between July  
251 and October [*Kivi et al.*, 2007 - Table 3]. In order to test for such seasonal trends in the ozone observations we  
252 further sub-divide the data shown in Figure 4 based upon day of year.

253

254 Figure 5 shows the same series of plots as shown in Figure 4, but this time the data are only shown for the  
255 months July, August, September, and October (JASO) - periods when the polar vortex is absent over northern  
256 Finland [*Kivi et al.*, 2007]. In comparison with Figure 4, it is clear that changes in ozone following SPEs during  
257 these months are practically absent. There are fluctuations around the mean level throughout the epoch period,  
258 but there is little evidence for any systematic decrease in ozone partial pressure during these SPEs.

259

260 Figure 6 shows the same series of plots as shown in Figure 4 and Figure 5, but here the data are only shown for  
261 the months January, February, March, and April (JFMA); periods when the polar vortex is frequently present  
262 over northern Finland (~50% of the time) and can cause more rapid descent of long-lived NO<sub>x</sub> during hours of  
263 darkness. In contrast with the plots in Figure 4 and Figure 5, it is clear that a large reduction in the stratospheric  
264 ozone partial pressure occurs immediately following SPE arrival at Earth. This reduction persists for many  
265 days. Again, the reduction in the running mean commences slightly prior to zero-epoch in the 15-day running  
266 average, although the individual (red) data points do not show evidence of a decrease until zero epoch. We also  
267 note that prior to zero-epoch the ozone for the SPE events is already greater than the mean value - this is due to  
268 the fact that the SPEs are more common during the years around solar maximum, when ozone levels tend to be  
269 slightly elevated. In general, years around solar maximum have higher ozone concentrations on average,  
270 although this trend clearly isn't true in all years. It is strongly -and- depends on other factors- that affecting the

271 production and the loss of ozone (e.g. catalytic loss of ozone in the springtime caused by ClO and BrO  
272 reactions) [cf. *Manney et al.*, 2011].

273

274 Clearly, the reduction in ozone commencing at zero epoch is significant, being of the order of 10% during  
275 JFMA when the polar vortex is active over northern Finland. A minimum decrease is reached ~8 days on  
276 average after the SPE and ozone remains at a level below the mean value for ~40 days, and continues to  
277 fluctuate beyond this time. This result supports the interpretation that destruction of stratospheric ozone is  
278 occurring, due to the external driver of solar-wind proton precipitation. ~~However, w~~While the reduction in  
279 measured stratospheric ozone following SPE-arrival is clearly evident in Figure 6, the descent of NO<sub>x</sub> in the  
280 polar vortex at these lower altitudes is quite slow: around 8 km/month at ~50 km altitude [*Manney et al.*, 1994;  
281 *Rinsland et al.*, 2005]. Hence, a more-gradual response in ~~the -ozonesonde-observations~~ ozone decrease  
282 might be expected, rather than a decrease immediately following SPE arrival at Earth. A delay in the  
283 destruction of ozone, due to NO<sub>x</sub> production via electron ~~precipitation~~precipitation, is also possible (e.g.:  
284 *Andersson et al.* [2014], *Randall et al.* [2015]).. Further studies are required to pin down the ultimate causes of  
285 the ozone depletion revealed here, and such studies are underway. Based on the literature, it is anticipated that  
286 these causes likely will include an admixture of direct and indirect physical mechanisms.

287

### 288 3.4 Stratospheric Ozone Changes During High-speed Solar-wind Streams (HSSs)

289

290 Stimulus for the work carried out in this manuscript originally arose from the knowledge that high-speed solar-  
291 wind streams (HSSs) are associated with enhanced activity in the Earth's magnetosphere and subsequently with  
292 large increases in energetic particle precipitation originating from the plasma sheet and/or radiation belts, noted  
293 by a number of authors (e.g. *Sandanger et al.*, [2007], *Longden et al.* [2008], *Rodger et al.* [2008], *Denton et al.*  
294 [2009], *Borovsky and Denton* [2009], *Morley et al.* [2012], *Kavanagh et al.* [2012], *Hendry et al.* [2013],  
295 *Clilverd et al.* [2013], *Blum et al.* [2015]). Although the energy spectrum during HSS-events is much softer  
296 than during SPEs there is still ongoing energetic particle precipitation, primarily due to relativistic (>1 MeV)  
297 electrons. Given the long-lived nature of HSSs such precipitation persists for much longer time intervals  
298 whether as continuous low-energy precipitation [*Whittaker et al.*, 2014;] or in the form of electron microbursts  
299 [*Nakamura et al.*, 2000; *Lorentzen et al.*, 2001; *Blum et al.*, 2015]. Indeed, ozone decreases in the middle  
300 atmosphere have been clearly observed during medium energy precipitation [*Andersson et al.*, 2014]. Using the

301 data set described above, a search for substantial changes in stratospheric ozone partial pressure in the days  
302 following HSS-arrival, including times when the polar vortex was active, was carried out. The results from that  
303 study proved inconclusive (figure not shown).

304

#### 305 **4. Discussion and Conclusions**

306

307 The analysis and results shown above highlight the difficulty in extracting changes in stratospheric ozone due to  
308 a single variable. However, by removing the monthly mean variations from the measured ozone partial  
309 pressure, and by concentrating on intervals when the polar vortex is active, and hence can assist in the descent of  
310 NO<sub>x</sub> species, it has been clearly demonstrated that solar protons are causing substantial stratospheric ozone  
311 depletion of the order of 10%, following SPEs. ~~We argue that such external driving of the Earth's stratospheric~~  
312 ~~ozone budget has been under-appreciated~~  
313 ~~to date.~~

314

315 Determination of ozone variability on the Earth's climate is of great topical interest although reviews of the  
316 behaviour of ozone throughout the atmosphere have tended to concentrate on internal terrestrial variables  
317 [Stahelin *et al.*, 2001], or long-term solar changes [Haigh, 2003]– rather than directly on short-term solar-  
318 induced forcing via SPEs. We argue that external driving of the Earth's stratospheric ozone budget was  
319 somewhat under-appreciated originally with studies initially concentrating on effects in the upper  
320 stratosphere and mesosphere [Rusch *et al.*, 1981; Solomon *et al.*, 1981; 1983]. Changes in the  
321 lower stratosphere due to external driving are now receiving more attention in the literature. Where ~~studies of~~  
322 solar-proton effects on climate are considered within global climate models, the effects have been reported as  
323 not statistically significant with regard to the annually averaged temperature and the total ozone variation (e.g.  
324 Jackman *et al.* [2009]). Although incorporation of the effects of short-term solar-proton fluctuations in global  
325 coupled climate models is currently quite rare, the effects of solar protons have been included in other  
326 modelling studies previously (e.g. Jackman and McPeters [1985]; Jackman *et al.* [1996]; Rodger *et al.* [2008]).  
327 SPEs have also been shown to produce local changes to stratospheric ozone on a case-by-case basis (e.g. Weeks  
328 *et al.* [1972]; Heath *et al.* [1977]; Thomas *et al.* [1983]; López-Puertas *et al.* [2005]; Seppälä *et al.* [2006];  
329 Seppälä *et al.* [2008]). However, since most energy is deposited above 40 km, the direct effects of SPEs in  
330 general have not been considered important for quantification of total global ozone losses (e.g. Sinnhuber *et al.*

331 [2003]), despite the long-lived nature of NO<sub>x</sub> species generated at higher altitudes allowing their descent to  
332 occur over a period of weeks or months (e.g. *Randall et al.* [2001]). The full effects of SPEs may not be  
333 appreciated by study of single events. In this study, superposed epoch analysis of 191 SPEs has enabled a  
334 longer-duration statistical investigation of the average changes in ozone partial pressures to be carried out. Our  
335 work emphasises the need to incorporate energetic particle precipitation into climate models and we  
336 acknowledge the recent efforts in this direction (e.g. *Matthes et al.* [2017]).

337

## 338 **5. Summary**

339

340 In summary, we have analyzed data from 1845 balloon ozonesondes launched from Sodankylä, northern  
341 Finland, between 1989 and 2015. The mean monthly variation of stratospheric ozone has been calculated. The  
342 data have been analysed with respect to a number of geophysical variables (the AE index, the F10.7 index, the  
343 solar wind electric field parameter, and the Dst index), although no direct correlations to between stratospheric  
344 ozone and these indices (with a 24 hour time lag) was found.

345

346 To the best of our knowledge, this is the first comprehensive statistical study using balloon ozonesonde data that  
347 has provided direct, and long-term, in-situ evidence for stratospheric ozone depletion by SPEs in the northern  
348 hemisphere.

349

350 The results from this study are:

351

352 1. The average stratospheric ozone measured over northern Finland is highly variable during the year. The  
353 mean of the ozone partial pressure is greatest in winter and early spring and minimised in summer and early  
354 autumn.

355

356 2. There is no clear evidence for direct correlations between the stratospheric ozone partial pressure and the AE  
357 index, the F10.7 index, the solar-wind electric field, or the Dst index measured on the previous day.

358

359 3. A superposed epoch analysis of 191 SPEs examined between 1989 and 2015 indicates a fall in the ozone  
360 partial pressure of ~5% with a minimum reached ~8 days (on average) after the SPE arrival. The ozone partial

361 pressure remains reduced below its mean value for ~40 days.

362

363 4. When only time intervals are considered when the polar vortex is present over northern Finland (i.e. late  
364 winter) the fall in ozone partial pressure is ~10% with the minimum again reached after ~8 days (on average)  
365 after SPE arrival. The ozone remains reduced below its mean value for ~40 days. In contrast, no decrease in  
366 ozone is found following SPEs that occur during the northern hemisphere summer months of July-October when  
367 the polar vortex is not present.

368

369 It is intended that this study will highlight the fact that the average stratospheric ozone reduction is significant  
370 (~10%) following SPEs during the northern polar winter. We also intend that this knowledge be utilised to  
371 separate anthropogenic causes of ozone loss from natural causes. As noted in Section 2, balloon ozonesonde  
372 data have the advantage over satellite data that they provide high spatial resolution altitude profiles of the ozone  
373 distribution throughout the lower stratosphere. We plan on future~~ther~~ analysis of other measured ozone data  
374 sources ~~will be carried out~~ to investigate if the above findings are truly global or local (i.e. polar latitudes only)  
375 in nature. A follow-up study, using the same methodology but utilizing global satellite data coupled with multi-  
376 station balloon ozonesonde data from inside and outside the polar vortex, would certainly address this issue.

377 In an era when separating anthropogenic ozone depletion from natural ozone depletion is receiving widespread  
378 attention, the results from this current study, summarised above, are particularly timely in that they provide  
379 quantification of the expected average ozone reduction for a number of events rather than quantifying such  
380 losses during single-event case-studies. Such averaged results should prove simpler to include in global climate  
381 models.

382

### 383 **Acknowledgements**

384 This work was supported at the Space Science Institute by the NASA Heliophysics LWS program via grants  
385 NNX14AN90G and NNX16AB75G, the NASA Heliophysics GI program via grant NNX14AC15G, and the  
386 NSF GEM program award number 1502947. Ozonesonde work at the FMI was supported by the Academy of  
387 Finland (grant number 140408); an EU Project GAIA-CLIM; the ESA's Climate Change Initiative programme  
388 and the Ozone\_cci subproject in particular. The work was originally conceived under the EU LAPBIAT II  
389 project (contract RITA-CT-2006-025969) and the authors gratefully acknowledge this support. MHD would  
390 like to thank Andrew Senior and Joe Borovsky for helpful comments and suggestions regarding data analysis,

391 and the magnetospheric consequences of SPEs and HSSs, respectively. MHD offers particular thanks to all at  
392 Sodankylä Geophysical Observatory and the Finnish Meteorological Institute for their gracious hospitality  
393 during his visits to Sodankylä in the spring of 2008, 2012, and 2017.

394

## 395 **References**

396

397 Andersson, M., P. T. Verronen, C. J. Rodger, M. A. Clilverd, and A. Seppälä, Missing driver in the Sun–Earth  
398 connection from energetic electron precipitation impacts mesospheric ozone, *Nature Comm.*, 5,  
399 doi:10.1038/ncomms6197, 2014.

400

401 Blum, L., X. Li, and M. Denton, Rapid MeV electron precipitation as observed by SAMPEX/HILT during high-  
402 speed stream-driven storms, *J. Geophys. Res. Space Physics*, 120, 3783–3794, 2015.

403

404 Borovsky, J. E., and M. H. Denton, Relativistic-electron dropouts and recovery: A superposed epoch study of  
405 the magnetosphere and the solar wind, *J. Geophys. Res.*, 114, A02201, doi:10.1029/2008JA013128, 2009.

406

407 Butchart, N., The Brewer-Dobson circulation, *Rev. Geophys.*, 52, doi:10.1002/2013RG000448, 2014.

408

409 Clilverd, M. A., N. Cobbett, C. J. Rodger, J. B. Brundell, M. H. Denton, D. P. Hartley, J. V. Rodriguez, D.  
410 Danskin, T. Raita, and E. L. Spanswick, Energetic electron precipitation characteristics observed from  
411 Antarctica during a flux dropout event, *J. Geophys. Res. Space Physics*, 118, doi:10.1002/2013JA019067, 2013.

412

413 Clilverd, M. A., C. J. Rodger, T. Ulich, A. Seppälä, E. Turunen, A. Botman, and N. R. Thomson, Modelling a  
414 large solar proton event in the southern polar atmosphere, *J. Geophys. Res.*, 110, A09307,  
415 doi:10.1029/2004JA010922, 2005.

416

417 Crutzen, P. J., I. S. A. Isaksen, and G. C. Reid, Solar proton events: Stratospheric sources of nitric oxide,  
418 *Science*, 189, 457-458, 1975.

419

420 [Damiani, A., M. Storini, M. Laurenza, and C. Rafanelli, Solar particle effects on minor components of the polar](#)  
421 [atmosphere, \*Ann. Geophys.\*, 26, 361–370, 2008.](#)  
422  
423 [Damiani, A., P. Diego, M. Laurenza, M. Storini and C. Rafanelli, Ozone variability related to several SEP](#)  
424 [events occurring during solar cycle no. 23, \*Adv. Space Res.\*, 43, 28-40, 2009.](#)  
425  
426 [Damiani, A., et al., Impact of January 2005 solar proton events on chlorine species, \*Atmos. Chem. Phys.\*, 12,](#)  
427 [4159–4179, 2012.](#)  
428  
429 Damiani, A., B. Funke, M. L. Puertas, M. L. Santee, R. R. Codero, and S. Watanabe, Energetic particle  
430 precipitation: A major driver of the ozone budget in the Antarctic upper stratosphere, *Geophys. Res. Lett.*, 43,  
431 3554-3562, 2016.  
432  
433 Davis, T. N., and M. Sugiura, Auroral electrojet activity index AE and its universal time variations, *J. Geophys.*  
434 *Res.*, 71(3), 785–801, 1966.  
435  
436 Denton, M. H., J. E. Borovsky, M. Stepanova, and J. A. Valdivia, Preface: Unsolved Problems of  
437 Magnetospheric Physics, *J. Geophys. Res.*, 121, 10,783–10,785, 2016.  
438  
439 Denton, M. H., T. Ulich, and E. Turunen, Modification of midlatitude ionospheric parameters in the F2 layer by  
440 persistent high-speed solar wind streams, *Space Weather*, 7, S04006, 2009.  
441  
442 Deshler, T., R. Stübi, F. J. Schmidlin, J. L. Mercer, H. G. J. Smit, B. J. Johnson, R. Kivi, and B. Nardi, Methods  
443 to homogenize ECC ozonsonde measurements across changes in sensing solution concentration or ozonsonde  
444 manufacturer, *Atmos. Meas. Tech. Discuss.*, doi:10.5194/amt-2016-415 (under review), 2017.  
445  
446 Deshler, T., J. L. Mercer, H. G. J. Smit, R. Stubi, G. Levrat, B. J. Johnson, S. J. Oltmans, R. Kivi, A. M.  
447 Thomson, J. Witte, J. Davies, F. J. Schmidlin, G. Brothers, and T. Sasaki, Atmospheric comparison of  
448 electrochemical cell ozonesondes from different manufacturers, and with different cathode solution strengths:  
449 The Balloon Experiment on Standards for Ozonesondes, *J. Geophys. Res.*, 113, D04307,

450 doi:10.1029/2007JD008975, 2008.

451

452 J. W. Gjerloev, R. A. Hoffman, M. M. Friel, L. A. Frank, J. B. Sigwarth. Substorm behavior of the auroral  
453 electrojet indices. *Annales Geophysicae*, European Geosciences Union, 2004, 22 (6), 2135-2149, 2004.

454

455 Haigh, J. D., The effects of solar variability on the Earth's climate, *Phil. Trans. R. Soc. Lond. A.*, 361, 95-111,  
456 2003.

457

458 Heath, D. F., A. J. Kruger, and P. J. Crutzen, Solar proton events: Influence on stratospheric ozone, *Science*,  
459 197, 886-889, 1977.

460

461

462 Hendry, A. T., C. J. Rodger, M. A. Clilverd, N. R. Thomson, S. K. Morley, T. Raita, Rapid radiation belt losses  
463 occurring during high-speed solar wind stream-driven storms: Importance of energetic electron precipitation, in  
464 *Dynamics of the Earth's Radiation Belts and Inner Magnetosphere*, *Geophys. Monogr. Ser.*, vol. 199, edited by  
465 D. Summers et al., 213–223, AGU, Washington, D. C., doi:10.1029/2012GM001299, 2013.

466

467 Hocke, K., Response of the middle atmosphere to the geomagnetic storm of November 2004, *J. Atmos. Sol-  
468 Terr. Phys.*, 154, 86-91, 2017.

469

470 Jackman, C. H., and R. D. McPeters, the response of ozone to solar proton events during solar cycle 21: A  
471 theoretical interpretation, *J. Geophys. Res.*, 90, 7955-7966, 1985.

472

473 Jackman, C. H., R. D. Marsh, F. M. Vitt, R. R. Garcia, C. E. Randall, E. L. Fleming, and S. M. Frith, Long-term  
474 middle atmospheric influence of very large solar proton events, *J. Geophys. Res.*, 114, D11304,  
475 doi:10.1029/2008JD011415, 2009.

476

477 Jackman, C. H., E. L. Fleming, S. Chandra, D. B. Considine, and J. E. Rosenfield, Past, present, and future  
478 modeled ozone trends with comparisons to observed trends, *J. Geophys. Res.*, 101, 28753-28767, 1996.

479

480 Jackman, C. H., M. C. Cerniglia, J. E. Nielsen, D. J. Allen, J. M. Zawodny, R. D. McPeters, A. R. Douglass, J.  
481 E. Rosenfield, and R. B. Hood, Two-dimensional and three-dimensional model simulations, measurements, and  
482 interpretation of the October 1989 solar proton events on the middle atmosphere, *J. Geophys. Res.*, 100, 11641-  
483 11660, 1995.

484

485 Kavanagh, A. J., F. Honary, E. F. Donovan, T. Ulich, and M. H. Denton, Key features of >30 keV electron  
486 precipitation during high speed solar wind streams: A superposed epoch analysis, *J. Geophys. Res.*, 117,  
487 A00L09, 2012.

488

489 King, J. H., and N. E. Papitashvili, Solar wind spatial scales in and comparisons of hourly Wind and ACE  
490 plasma and magnetic field data. *J. Geophys. Res.*, 110, A02209, doi:10.1029/2004JA010804, 2005.

491

492 Kivi, R., E. Kyrö, T. Turunen, N. R. P. Harris, P. von der Gathen, M. Rex, S. B. Anderson, and I. Wohltmann,  
493 Ozonesonde observations in the Arctic during 1989-2003: Ozone variability and trends in the lower stratosphere  
494 and free troposphere, *J. Geophys. Res.*, 112, D08306, doi:10.1029/2006JD007271, 2007.

495

496 Kurt, V., A. Belov, H. Mavromichalaki, and M. Gerontidou, Statistical analysis of solar proton events, *Ann.*  
497 *Geophys.*, 22, 2255–2271, 2004.

498

499 Longden, N., M. H. Denton, and F. Honary, Particle precipitation during ICME-driven and CIR-driven  
500 geomagnetic storms, *J. Geophys. Res.*, 113, A06205, 2008.

501

502 López-Puertas, M., B. Funke, S. Gil-Lopéz, T. V. Clarmann, G. P. Stiller, M. Höpfner, S. Kellmann, H. Fischer,  
503 and C. H. Jackman, Observation of NO<sub>x</sub> enhancement and ozone depletion in the Northern and Southern  
504 hemispheres after the October-November 2003 solar proton events, *J. Geophys. Res.*, 110, A09S43,  
505 doi:10.1029/2005JA011050, 2005.

506

507 Lorentzen, K.R., Looper, M.D., Blake, J. B., Relativistic electron microbursts during the GEM storms,  
508 *Geophys. Res. Lett.*, 28, 2573, 2001.

509

510 Matthes, Funke, Andersson, Barnard, Beer, Charbonneau, Clilverd, Dudok de Wit, Haberreiter, Hendry,  
511 ackman, Kretzschmar, Kruschke, Kunze, Langematz, Marsh, Maycock, Misios, Rodger, Scaife, Seppälä,  
512 Shangguan, Sinnhuber, Tourpali, Usoskin, van de Kamp, Verronen, and Versick, Solar Forcing for CMIP6,  
513 Geoscientific Model Development, doi:10.5194/gmd-2016-9, ([in oressunder review](#)), 2017.  
514

515 Manney, G. L., Santee, M. L., Rex, M., Livesey, N. J., Pitts, M. C., Veefkind, P., Nash, E. R., Wohltmann, I.,  
516 Lehmann, R., Froidevaux, L., Poole, L. R., Schoeberl, M. R., Haffner, D. P., Davies, J., Dorokhov, V.,  
517 Gernandt, H., Johnson, B., Kivi, R., Kyro, E., Larsen, N., Levelt, P. F., Makshtas, A., McElroy, C. T.,  
518 Nakajima, H., Parrondo, M. C., Tarasick, D. W., von der Gathen, P., Walker K. A., and Zinoviev, N. S.:  
519 Unprecedented Arctic Ozone loss in 2011, *Nature*, 478, 469–475, 2011.  
520

521 Manney, G. L., R. W. Zurek, A. O'Neil, and R. Swinbank, On the motion of air through the stratospheric polar  
522 vortex, *J. Atmos. Sci.*, 51, 2973 – 2994, 1994.  
523

524 Morley, S. K., R. H. W. Friedel, T. E. Cayton, and E. Noveroske, A rapid, global and prolonged electron  
525 radiation belt dropout observed with the Global Positioning System constellation, *Geophys. Res. Lett.*, 37,  
526 L06102, 2010.  
527

528 Nakamura, R., Isowa, M., Kamide, Y., Baker, D.N., Blake, J.B., Looper, M., SAMPEX observations of  
529 precipitation bursts in the outer radiation belt, *J. Geophys. Res.*, 105, 15875, 2000.  
530

531 Oh, S. Y., Y. Yi, J. W. Bieber, P. Evenson, and Y. K. Kim, Characteristics of solar proton events associated  
532 with ground level enhancements, *J. Geophys. Res.*, 115, A10107, 2010.  
533

534 Park, S. K., and K. W. Miller, Random Number Generators: Good Ones are Hard to Find, *Communications of*  
535 *the ACM*, Vol. 31, No. 10, p. 1192-1201, 1988.  
536

537 [Randall, C. E., V. L. Harvey, L. A. Holt, D. R. Marsh, D. E. Kinnison, B. Funk and P. F. Bernath, Simulation of](#)  
538 [energetic particle precipitation effects during the 2003-2004 Arctic winter, \*Journal of Geophysical Research :\*](#)  
539 [Space Physics, 120, 5035–5048, doi:10.1002/2015JA021196, 2015.](#)

540

541 Randall, C. E., D. E. Siskind, and R. M. Bevilaqua, Stratospheric NO<sub>x</sub> enhancements in the southern hemisphere  
542 vortex in winter/spring of 2000, *Geophys. Res. Lett.*, 28, 2385-2388, 2001.

543

544 Reames, D. V., Particle acceleration at the Sun and in the heliosphere, *Space Sci. Rev.*, 90, 413–491, 1999.

545

546 Rinsland, C. P., C. Boone, R. Nassar, K. Walker, P. Bernath, J. C. McConnell, and L. Chiou, Atmospheric  
547 Chemistry Experiment (ACE) Arctic stratospheric measurements of NO<sub>x</sub> during February and March 2004:  
548 Impact of intense solar flares, *Geophys. Res. Lett.*, 32, L16S05, 2005.

549

550 Rodger, C. J., P. T. Verronen, M. A. Clilverd, A. Seppälä, and E. Turunen, Atmospheric impact of the  
551 Carrington event solar protons, *J. Geophys. Res.*, 113, D23302, doi:10.1029/2008JD010702, 2008.

552

553 Rodger, C. J., M. A. Clilverd, J. C. Green, and M. M. Lam, Use of POES SEM-2 observations to examine  
554 radiation belt dynamics and energetic electron precipitation into the atmosphere, *J. Geophys. Res.*, 115, A04202,  
555 2010.

556

557 Rodger, C. J., M. A. Clilverd, P. T. Verronen, Th. Ulich, M. J. Jarvis, and E. Turunen, Dynamic geomagnetic  
558 rigidity cutoff variations during a solar proton event, *J. Geophys. Res.*, 111, A04222,  
559 doi:10.1029/2005JA011395, 2006.

560

561 [Rusch, D. W., J.-C. Gérard, S. Solomon, P. J. Crutzen, and G. C. Reid, The effect of particle precipitation events  
562 on the neutral and ion chemistry of the middle atmosphere: I. Odd nitrogen, \*Planet. Space Sci.\*, 29\(7\), 767, 1981.](#)

563

564 Ryan, N. J., K. A. Walker, U. Raffalski, R. Kivi, J. Gross, and G. L. Manney, Ozone profiles above Kiruna  
565 from two ground-based radiometers, *Atmos. Meas. Tech.*, (under review), 2017.

566

567 Sandanger, M., F. Søråas, K. Aarsnes, K. Oksavik, and D. S. Evans, Loss of relativistic electrons: Evidence for  
568 pitch angle scattering by electromagnetic ion cyclotron waves excited by unstable ring current protons, *J.*  
569 *Geophys. Res.*, 112, A12213, doi:10.1029/2006JA012138, 2007.

570

571 Sckopke, N., A general relation between the energy of trapped particles and the disturbance field near the earth,  
572 J. Geophys. Res., 71, 3125, 1966.

573

574 Seppälä, A., C. E. Randall, M. A. Clilverd, E. Rozanov, and C. J. Rodger, Geomagnetic activity and polar  
575 surface air temperature variability, J. Geophys. Res., 114, A10312, doi:10.1029/2008JA014029, 2009.

576

577 Seppälä, A., M. A. Clilverd, C. J. Rodger, P. T. Verronen, and E. Turunen, The effects of hard-spectra solar  
578 proton events on the middle atmosphere, J. Geophys. Res., 113, A11311, doi:10.1029/2008JA013517, 2008.

579

580 Seppälä, A., P. T. Verronen, V. F. Sofieva, J. Tamminen, E. Kyrölä, C. J. Rodger, and M. A. Clilverd,  
581 Destruction of the tertiary ozone maximum during a solar proton event, Geophys. Res. Lett., 33, L07804,  
582 doi:10.1029/2005GL025571, 2006.

583

584 Seppälä, A., P. T. Verronen, E. Kyrölä, S. Hassinen, L. Backman, A. Hauchecorne, J. L. Bertaux, and D.  
585 Fussen, Solar proton events of October–November 2003: Ozone depletion in the Northern Hemisphere polar  
586 winter as seen by GOMOS/Envisat, Geophys. Res. Lett., 31, L19107, 2004.

587

588 Sinnhuber, M., J. P. Burrows, M. P. Chipperfield, C. H. Jackman, M-B. Kallenrode, K. F. Künzi, and M. Quack,  
589 A model study of the impact of magnetic field structure on atmospheric composition during solar proton events,  
590 Geophys. Res. Lett., 30, 15, 1818, doi:10.1029/2003GL017265, 2003.

591

592 Shumilov, O. I., E. A. Kasatkina, V. A. Turyansky, E. Kyrö, and R. Kivi, Solar cosmic ray effects in  
593 atmospheric chemistry evidenced from ground-based measurements, Adv. Space Res., 31, 9, 2157-2162, 2003.

594

595 Smit, H. G. J. and the ASOPOS panel (Assessment of Standard Operating Procedures for Ozonesondes):  
596 Quality assurance and quality control for ozonesonde measurements in GAW, World Meteorological  
597 Organization, GAW Report #201, Geneva, Switzerland, 2014. available at:  
598 [http://www.wmo.int/pages/prog/arep/gaw/documents/FINAL\\_GAW\\_201\\_Oct\\_2014.pdf](http://www.wmo.int/pages/prog/arep/gaw/documents/FINAL_GAW_201_Oct_2014.pdf).

599

600 Solomon, S., D. W. Rusch, J. C. Gérard, G. C. Reid, and P. Crutzen, The effect of particle precipitation on the  
601 neutral and ion chemistry of the middle atmosphere: II odd hydrogen, *Planet. Space Sci.*, 29, 885-892, 1981.

602

603 [Solomon, S., D. W. Rusch, R. J. Thomas, and R. S. Eckman, Comparison of mesospheric ozone abundance](#)  
604 [measured by the Solar Mesosphere Explorer and model calculations, \*Geophys. Res. Lett.\*, 10, 249-252,](#)  
605 [doi:10.1029/GL010i004p00249, 1983.](#)

606

607 Staehelin, J., N. R. P. Harris, C. Appenzeller, and J. Eberhard, Ozone trends: A review, *Rev. Geophys.*, 39, 231-  
608 290, 2001.

609

610 Tapping, K. F., The 10.7 cm solar radio flux ( F 10.7 ), *Space Weather*, 11, 394-406, 2013.

611

612 Thomas, R. J., C. A. Barth, G. J. Rottman, D. W. Rusch, G. H. Mount, G. M. Lawrence, R. W. Sanders, G. E.

613 Thomas, L. E. Clemens, Mesospheric ozone depletion during the solar proton event of July 13, 1982: Part 1  
614 Measurement, *Geophys. Res. Lett.*, 10, 253-255, 1983.

615

616 Turunen, E., A. Kero, P. T. Verronen, Y. Miyoshi, S.-I. Oyama, and S. Saito, Mesospheric ozone destruction by  
617 high-energy electron precipitation associated with pulsating aurora, *J. Geophys. Res. Atmos.*, 121,  
618 doi:10.1002/2016JD025015, 2016.

619

620 Tylka, A. J., C. M. S. Cohen, W. F. Dietrich, M. A. Lee, C. G. MacLennan, R. A. Mewaldt, C. K. Ng, and D. V.  
621 Reames, A comparative study of ion characteristics in the large gradual solar energetic particle events of 2002  
622 April 21 and 2002 August 24, *Astrophys. J. Suppl. Ser.*, 164, 536-551, 2006.

623

624

625 [Verronen, P. T., and R. Lehmann, Analysis and parameterisation of ionic reactions affecting middle atmospheric](#)  
626 [HOx and NOy during solar proton events, \*Ann. Geophys.\*, 31, 909-956, doi:10.5194/angeo-31-909-2013, 2013.](#)

627

628 Verronen, P. T., M. L. Santee, G. L. Manney, R. Lehmann, S.-M. Salmi, and A. Seppala, Nitric acid  
629 enhancements in the mesosphere during the January 2005 and December 2006 solar proton events, *J. Geophys.*

630 Res., 116, D17301, 2011.

631

632 Sugiura, M., Hourly values of equatorial Dst for the IGY, *Ann. Int. Geophys. Year*, 35, 9, Pergamon Press,  
633 Oxford, 1964.

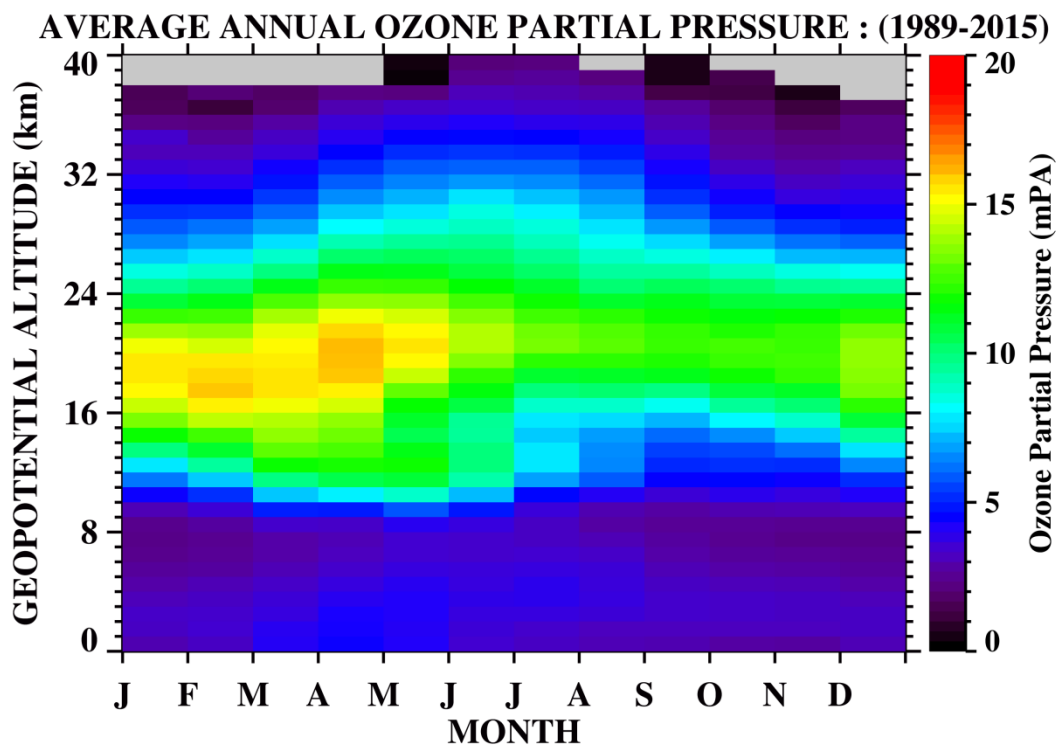
634

635 Weeks, L. H., R. S. CuiKay, and J. R. Corbin, Ozone measurements in the mesosphere during the solar proton  
636 event of 2 November 1969, *J. Atmos. Sci.*, 29, 1138-1142, 1972.

637

638 Whittaker, I. C., M. A. Clilverd, and C. J. Rodger, Characteristics of precipitating energetic electron fluxes  
639 relative to the plasmopause, *J. Geophys. Res.*, 119, 8784–8800, doi:10.1002/2014JA020446, 2014.

640

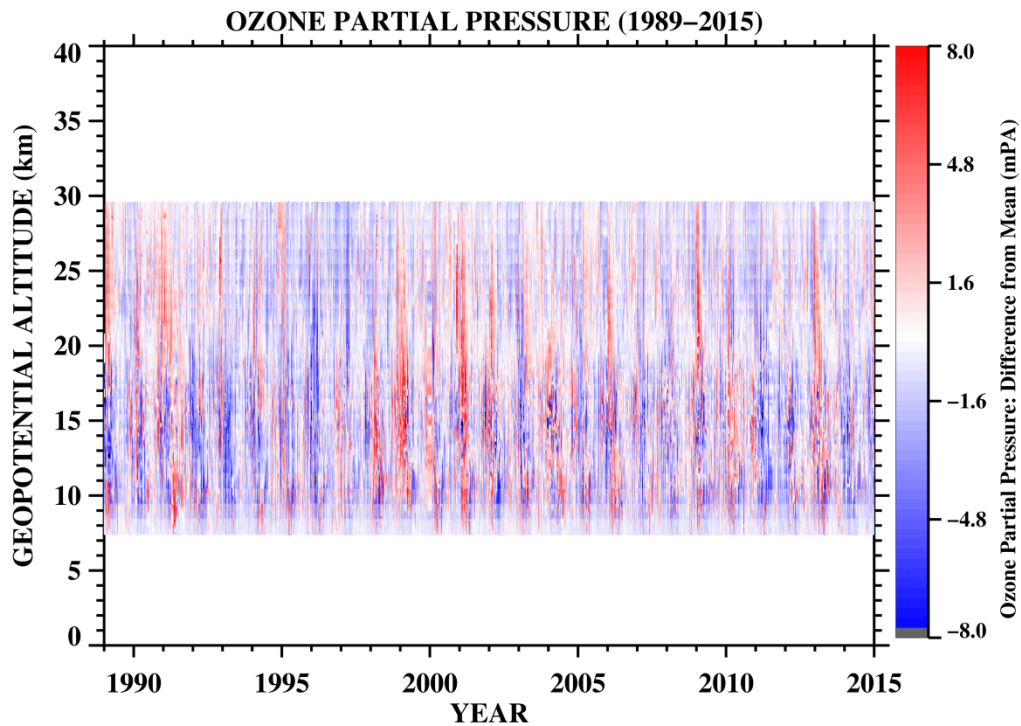
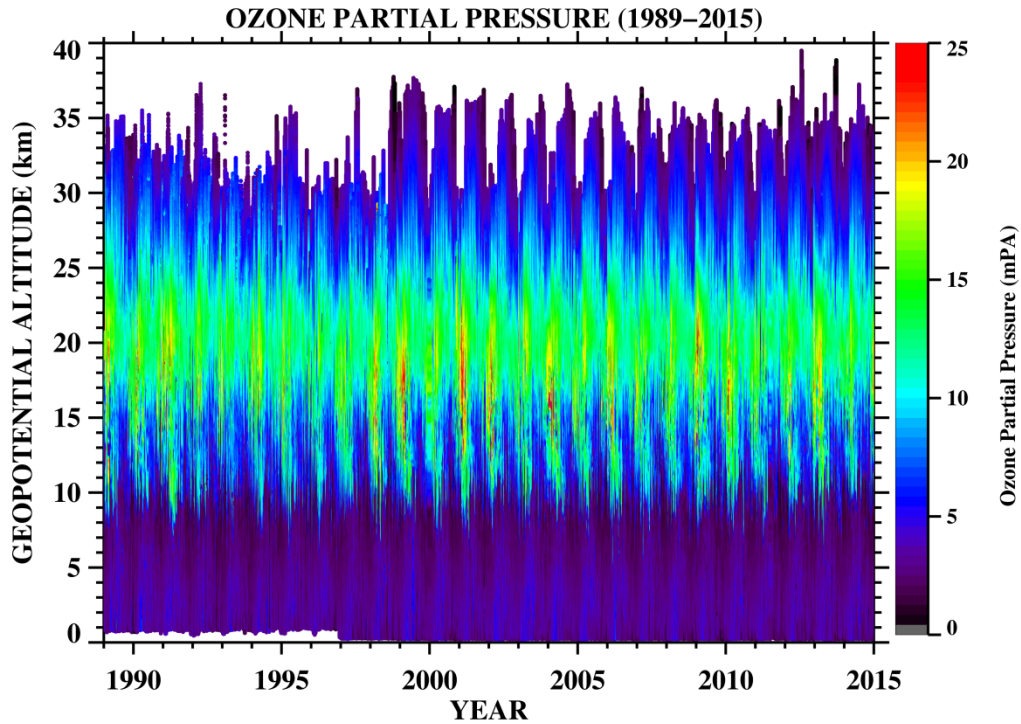


642

643

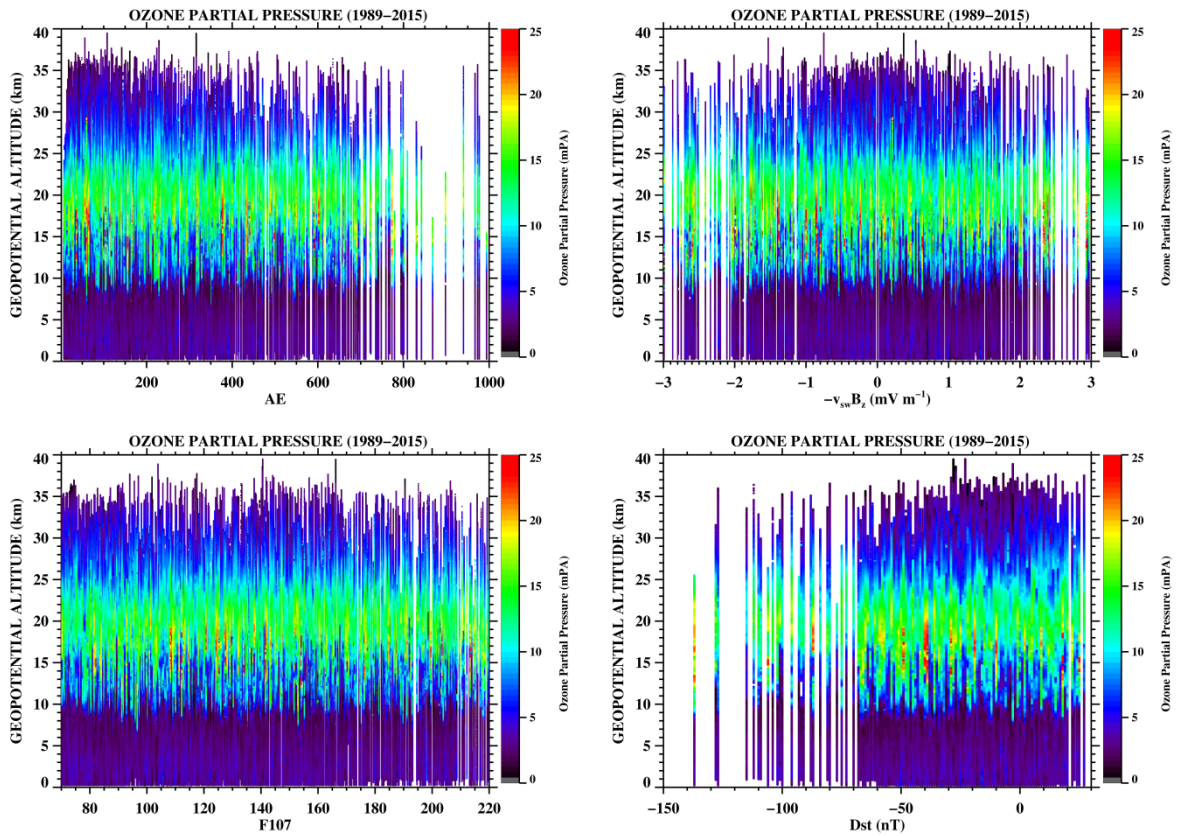
644 **FIGURE 1:** The averaged ozone partial pressure (in mPa) as a function of geopotential altitude and month-of-  
 645 the-year for 1845 balloon ozonesondes launched between 1989 and 2015 from Sodankylä, northern Finland.  
 646 Ozone is higher in winter/early-spring months and lower in summer/autumn months. (Note: This analysis  
 647 updates the previous analysis of *Kivi et al.* [2007], Figure 4).

648



650

651 **FIGURE 2:** Showing a time-series of all ozonesonde data from Sodankylä between 1989 and 2015. The top  
 652 plot shows the ozone partial pressure as a function of year and geopotential altitude. The bottom figure shows  
 653 the same data (8-30 km altitude only), but this time adjusted for the seasonal mean variations using the data  
 654 from Figure 1. Positive values (red) indicate measurements that are higher than the long-term mean and  
 655 negative (blue) values show measurements that are lower than the long-term mean.



656

657

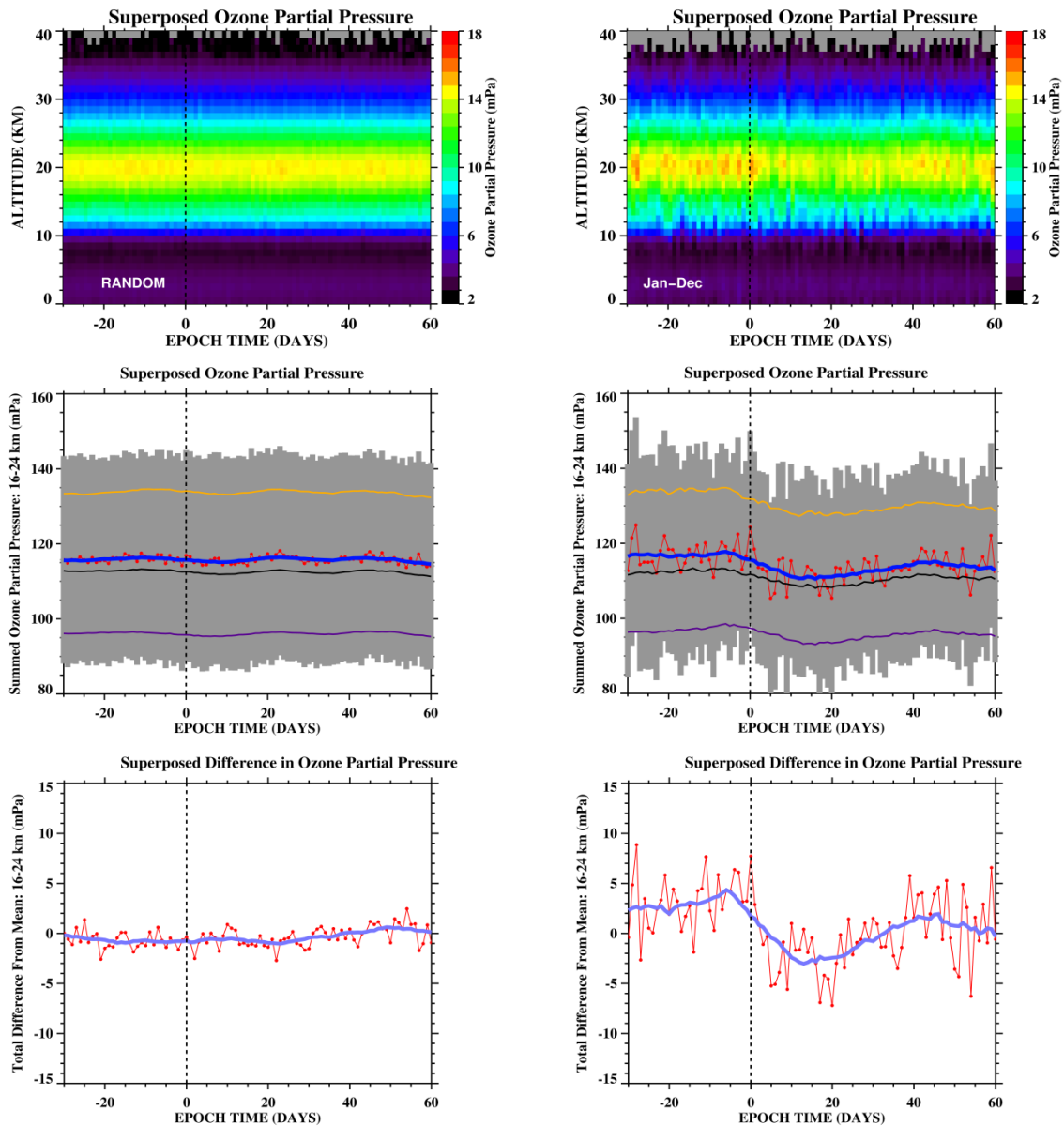
**FIGURE 3:** Plots showing the variation of the ozone partial pressure as a function of geopotential altitude in kilometres with (i) the AE index, (ii) the solar-wind electric field parameter  $-v_{sw}B_z$ , (iii) the F10.7 index, and (iv) the Dst index. There is little evidence for systematic changes in the ozone partial pressure with any of these four parameters.

658

659

660

661



663

664

**FIGURE 4:** Showing the ozone partial pressure as a function of geopotential altitude and epoch time for (a)

665

2500 random epochs selected between 1989 and 2015 (left column), and (b) 191 solar proton events that

666

occurred during the same interval (right column). The plots show the averaged ozone partial pressure up to 40

667

km altitude (top row), the integral of the ozone partial pressure between 16 and 24 km altitude (middle row), and

668

the integrated difference-from-mean quantity, also between 16 and 24 km altitude (note: -date become sparse in

669

for altitudes >~35km). The red points represent the individual data and the blue line is a 15-day running box-car

670

average for these data. The grey shading indicates the standard deviation of the superposition, whilst the thin

671

orange, black, and purple lines represent the upper quartile, the median, and the lower quartile of the

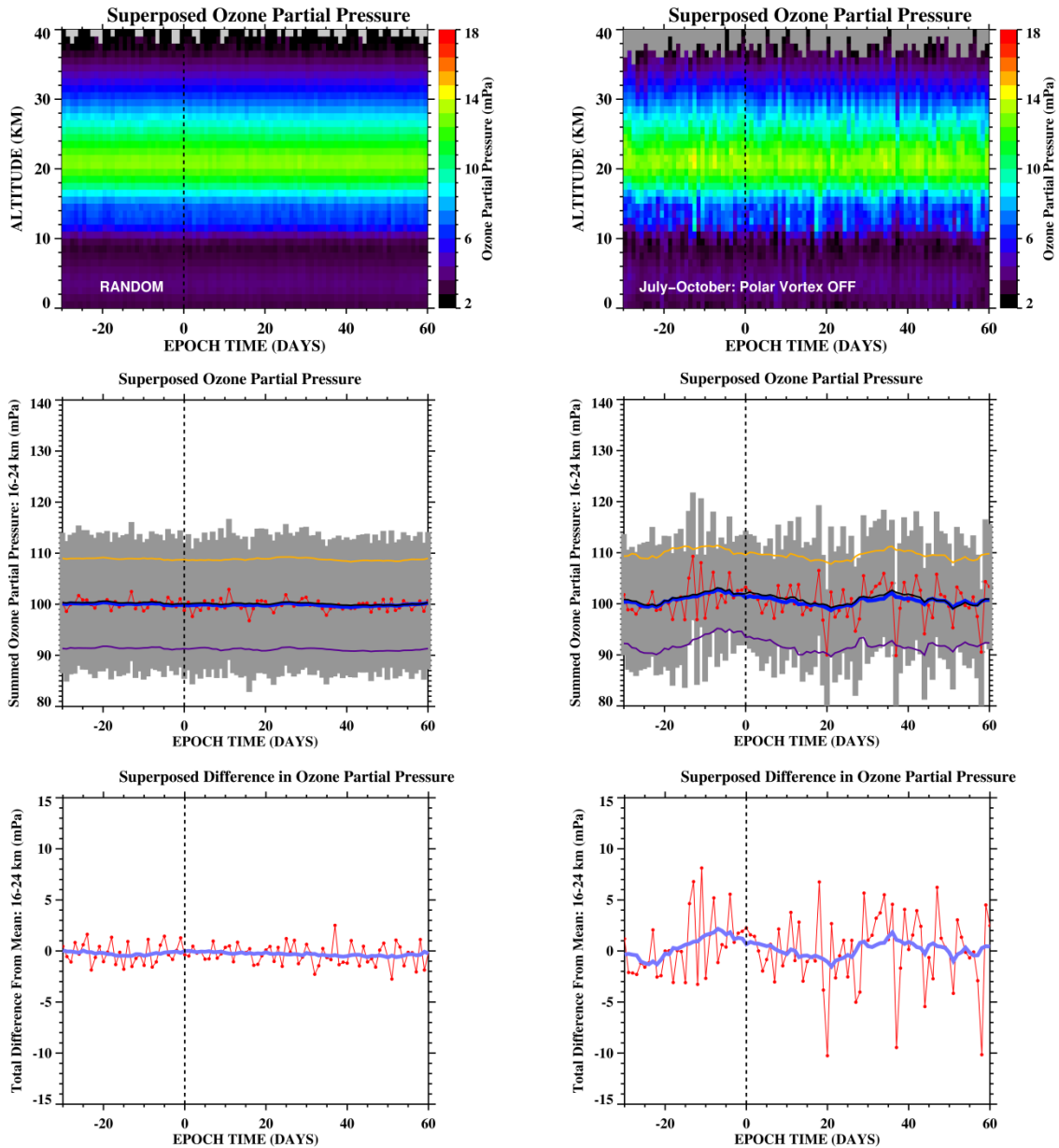
672

superpositions. There is a clear decrease in the ozone partial pressure following the arrival of solar proton

673

events.





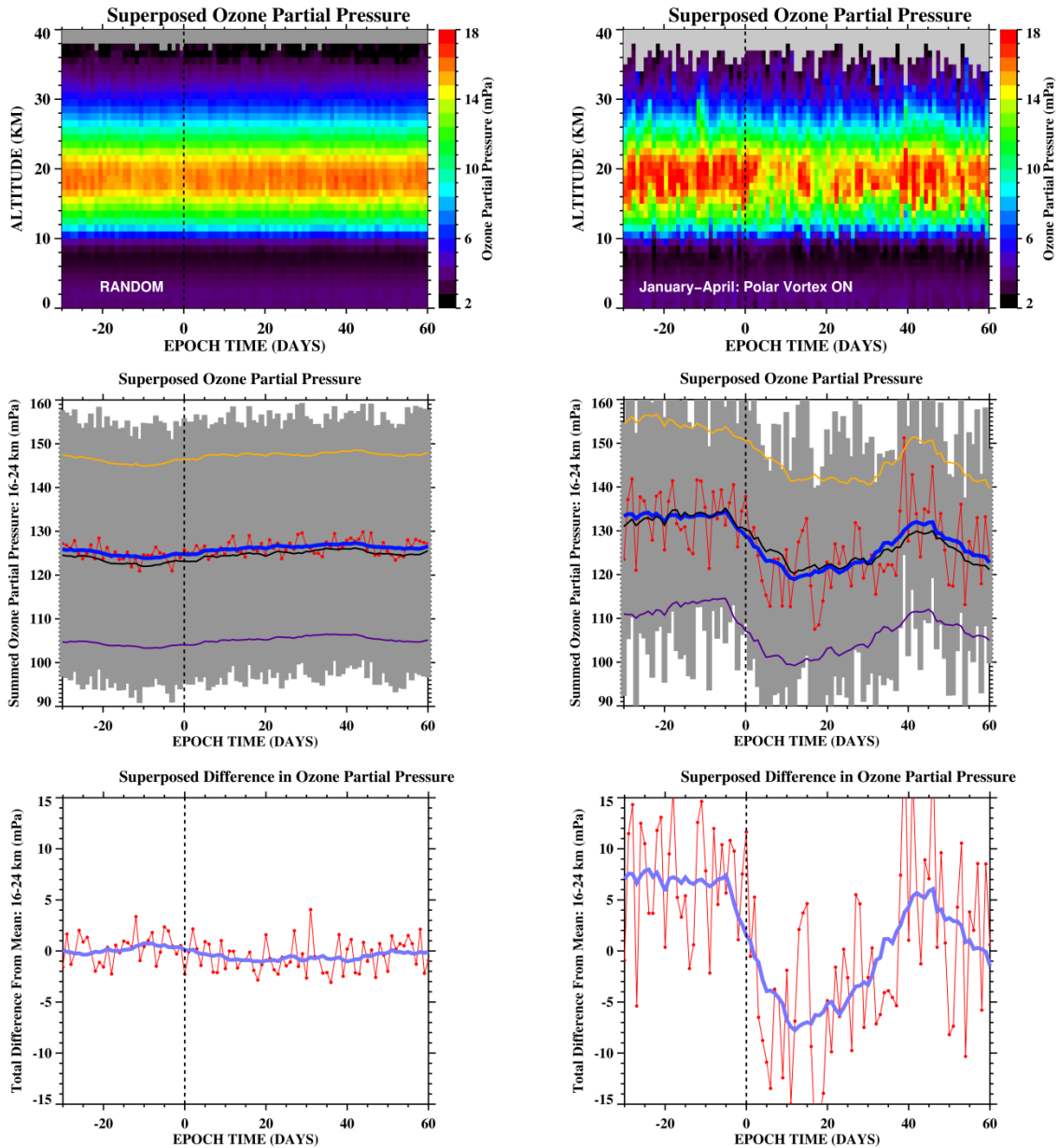
675

676

**FIGURE 5:** The same format as shown in Figure 4, but here data are only plotted for July, August, September, and October when the polar vortex is INACTIVE over Northern Finland. There is no clear trend for changes in the stratospheric ozone population following the SPEs.

678

679



681

682

**FIGURE 6:** The same format as shown in Figure 4 and Figure 5, but here data are only plotted for January, February, March and April, when the polar vortex is ACTIVE over Northern Finland. There is a clear trend for a decrease in the stratospheric ozone population following the SPEs.

684

685

## **HIGHLIGHTS:**

- No link between stratospheric ozone and geophysical indices (24 h lag)
- Stratospheric ozone falls ~10% after solar proton events - below mean for ~40 days.
- Ozone decrease only occurs during polar winter months, no effect in summer.

# Solar proton events and stratospheric ozone depletion over northern

## Finland

*M. H. Denton<sup>1,2</sup>, R. Kivi<sup>3</sup>, T. Ulich<sup>4</sup>, C. J. Rodger<sup>5</sup>, M. A. Clilverd<sup>6</sup>, R. B. Horne<sup>6</sup>, A. J. Kavanagh<sup>6</sup>.*

1. Space Science Institute, Boulder, CO 80301, USA.

2. New Mexico Consortium, Los Alamos, NM 87544, USA.

3. Arctic Research Centre, Finnish Meteorological Institute, Sodankylä, Finland.

4. Sodankylä, Geophysical Observatory, Sodankylä, Finland.

5. Department of Physics, University of Otago, New Zealand.

6. British Antarctic Survey (NERC), Cambridge, UK.

### ABSTRACT:

We examine the variation of stratospheric ozone over northern Finland using ozonesonde observations from 1845 stratospheric balloon flights launched between 1989 and 2015 from near Sodankylä. The annual variation of the ozone partial pressure is examined and seasonal variations are explored and quantified. Direct links between the measured ozone partial pressure and common solar-wind parameters are also examined. A superposed-epoch analysis of the observations based on 191 solar proton events (SPEs) reveals a clear drop in the ozone partial pressure that commences following SPE-arrival at Earth. This analysis shows a reduction in stratospheric ozone in the winter/early-spring months (when the polar vortex is active over northern Finland), in contrast to summer/early-autumn months where no decrease is detected. By subtracting the natural seasonal variations in ozone partial pressure the SPE-driven reduction in ozone between 16 km and 24 km altitude is quantified. Analysis indicates that the ozone partial pressure during winter/early-spring is reduced, with a minimum reached ~8 days following the SPE arrival. On average, the ozone partial pressure is reduced by ~10% between 16-24 km altitude and takes ~40 days to return to its previous level. To the best of our knowledge, this is the first comprehensive statistical study, on a regional basis, that provides direct, and long-term in-situ evidence for ozone depletion by SPEs in the northern hemisphere.

CORRESPONDING AUTHOR: M. H. Denton ([mdenton@spacescience.org](mailto:mdenton@spacescience.org))

## 31 1. Introduction

32 Solar proton events (SPEs) arise in association with energetic events on the Sun and energisation processes in  
33 interplanetary space (e.g. *Reames* [1999]; *Kurt et al.* [2004], *Tylka et al.* [2006], *Oh et al.*, [2010], and  
34 references therein). Upon arrival at Earth the solar protons may enter the upper atmosphere and collide with  
35 neutral particles at altitudes that are dependent on the incident energy of the protons [*Seppälä et al.*, 2008]. At  
36 this point they induce chemical changes to the local neutral population. Such energetic particle precipitation  
37 (EPP) is regularly implicated in the production of species such as odd nitrogen ( $\text{NO}_x$ ) (e.g. *Crutzen et al.* [1975];  
38 *Shumilov et al.* [2003]; *Clilverd et al.* [2005]), which are themselves implicated in the subsequent depletion of  
39 stratospheric ozone. Odd-nitrogen species are long-lived during darkness and can descend to stratospheric  
40 altitudes via the high-latitude polar vortex, during the polar winter. Once at stratospheric altitudes  $\text{NO}_x$  may  
41 cause chemical destruction of the in-situ ozone (e.g. *Jackman et al.* [1995]; *Jackman et al.* [2009]). Other  
42 chemical pathways for ozone destruction are also available (e.g. *Jackman et al.* [2009]; *Damiani et al.* [2008,  
43 2009, 2012]). Observational case studies of large individual SPEs reveal that such ozone depletions (in the  
44 mesosphere and stratosphere) do indeed occur (e.g. *Weeks et al.* [1972]; *Heath et al.* [1977]; *Thomas et al.*  
45 [1983]; *López-Puertas et al.* [2005]; *Seppälä et al.* [2004; 2006; 2008]). Modelling studies of such events have  
46 also helped ascertain the long and short term implications for atmospheric ozone balance (e.g. *Jackman and*  
47 *McPeters* [1985]; *Jackman et al.* [1996]; *Rodger et al.* [2008]; *Jackman et al.* [2009]). More general recent  
48 studies of the effects of EPP have outlined some of the chemical changes that occur during SPEs (e.g. *Verronen*  
49 *and Lehman* [2013]) and also recently drawn links between geomagnetic activity, particle precipitation, and  
50 changes in polar surface air temperature [*Seppälä et al.*, 2009]. However, a complete accounting of the  
51 chemical changes in the atmosphere resulting from EPP, and their relative importance, remains a major  
52 unsolved issue in magnetospheric and atmospheric physics [*Denton et al.*, 2016].

53  
54 In the current study we aim to expand upon current knowledge by using a large database of ozone measurements  
55 constructed from 1845 *ozonesonde* balloon flights, launched from Sodankylä in northern Finland, between 1989  
56 and 2015 [*Kivi et al.*, 2007]. Initially, these data are analysed to examine the seasonal/annual changes that occur  
57 in the ozone partial pressure in this region. Following this, links between the stratospheric ozone partial  
58 pressure and various common solar-wind parameters are explored. Subsequently, we carry out a statistical  
59 analysis of SPE-induced changes in stratospheric ozone during 191 SPE events that took place over the same  
60 time period as the ozonesonde observations. Finally, we quantify the observed reductions measured in the

61 ozone partial pressure following SPEs and discuss the implications of our findings, in comparison with other  
62 reported observations.

63

## 64 **2. Ozonesonde Data Set**

65 The ozone profiles used in this study were obtained by the electrochemical concentration cell (ECC) type of  
66 ozonesonde [Deshler *et al.*, 2008; 2017, Kivi *et al.*, 2007, Smit and ASOPOS Panel, 2014]. These instruments  
67 are capable of providing profile measurements of ozone concentration from the surface to the lower stratosphere  
68 (~30-34 km) with precision better than 2-3 % [Deshler *et al.*, 2008]. Vertical resolution of the soundings is  
69 about 10 meters, as data is typically analyzed in 2 second intervals, while the effective vertical resolution is of  
70 the order of 100-150 meters, given that the sensor response time is 20-30 seconds. The sondes used in this study  
71 have been launched on a regular basis from Sodankylä, Finland (67.4 N, 26.6 E) since 1989 during all seasons.  
72 Sondes are normally launched once per week around local noon. These data are supplemented by the frequent  
73 ozonesonde campaigns that have taken place in winter/spring season, significantly increasing the number of  
74 launches and the available dataset. This measurement program has resulted in 1845 soundings over the 27-year  
75 time period studied here. Balloon ozonesonde data have the advantage over satellite data that they provide high  
76 spatial resolution altitude profiles of the ozone distribution throughout the lower stratosphere. However, while  
77 these data are certainly suitable for study of changes in the ozone distribution over northern Finland, it should be  
78 noted that results will only apply on a local/regional basis. The details of the ozonesonde sounding system and  
79 principles of the data set homogenization are explained in detail in Kivi *et al.* [2007].

80

## 81 **3. Analysis and Results**

82

### 83 **3.1 Seasonal and Annual Variations of Stratospheric Ozone**

84

85 As previously shown by Kivi *et al.* [2007], there is a substantial annual variation in the stratospheric ozone  
86 partial pressure over Sodankylä during the year with a peak ozone level occurring around April and a minimum  
87 occurring around September (see Kivi *et al.* [2007], Figure 4). The annual cycle of ozone in the Arctic lower  
88 stratosphere is caused by the global annual cycle in ozone transport from lower latitudes towards the poles (e.g.  
89 Butchart, [2014], and references therein). This transport is strongest in winter and early spring and the ozone  
90 variability is highest during this period. The stratospheric ozone concentrations in late spring and summer

91 decrease continuously at high latitudes since the combination of ozone production and transport are too slow to  
92 offset the destruction of ozone via reactions involving  $\text{NO}_x$ . Significant destruction of ozone also occurs during  
93 via catalytic reactions involving chlorine monoxide (ClO) and bromine monoxide (BrO), but only during  
94 periods of sunlight (i.e. not during the polar winter) (e.g. *Jackman et al.* [2009]; *Damiani et al.* [2008, 2009,  
95 2012]). To take account of the annual and seasonal variability of ozone in our analysis, we initially extend the  
96 analysis of *Kivi et al.* [2007], who calculated the average monthly variation of stratospheric ozone between 1989  
97 and 2003. Here, this calculation is extended, using a further twelve years of data to cover the years 1989 to  
98 2015 inclusive (cf. Section 3.3).

99  
100 The average ozone partial pressure (in mPa) is calculated as a function of geopotential altitude (in km) and  
101 month of the year, for the entire ozonesonde dataset between 1989 and 2015. The results of this analysis are  
102 shown in Figure 1. (Note: As is common with sonde data we use geopotential altitude (height) rather than  
103 pressure units on the y-axis - the geopotential altitude approximates the altitude above sea-level of a particular  
104 pressure level). Clearly there is significant variability in the measured ozone on an inter-annual basis, which is  
105 largely due to inter-annual variability in chemical and dynamical factors influencing ozone. This inter-annual  
106 variability is strongly pronounced in the northern hemisphere, where dynamical variability is relatively large  
107 from year to year in contrast to the Antarctic stratosphere. However, significant vortex ozone depletions have  
108 also been observed in the northern hemisphere [*Manney et al.*, 2011].

109  
110 To explore the annual variations in the ozone data we examine the entire dataset of balloon-borne ozonesonde  
111 measurements made above northern Finland between 1989 and 2015, plotted in Figure 2 (top panel). It is clear  
112 that the regular seasonal variations (cf. Figure 1) are a prominent feature in this dataset, but there are also large  
113 changes on a year-to-year basis. For example, the measurements around 2001, close to solar maximum, are  
114 noticeably higher than most other periods.

115  
116 To quantify these changes we also plot these data on a seasonally-adjusted *difference-from-mean* basis (Figure  
117 2, bottom panel). The mean ozone partial pressure for the appropriate month and altitude (i.e. from the data  
118 shown in Figure 1) is subtracted from each individual measured ozone point in the data set. Doing this should  
119 remove seasonal trends from the data and allow variations due to other causes to be detected. The *seasonally-*  
120 *adjusted* difference-from-mean parameter plotted in Figure 2 provides quantification of the strength of the

121 variations on an annual basis. For example, for the data around 2001, the measured ozone is at times ~8 mPa  
122 higher than the mean value (at around 20 km altitude). In contrast, the measured ozone partial pressure is at  
123 times ~8 mPa lower than its mean value in 1993 (at around 15 km altitude). The years around solar maximum  
124 (when the solar EUV flux and F10.7 index are higher) show evidence of generally higher ozone levels compared  
125 to the years around solar minimum (when the solar EUV flux and F10.7 index are lower). However, this  
126 certainly isn't always true in every year with elevated F10.7 and there is much variation. The causes of annual  
127 variations are also known to include: (i) "internal" terrestrial effects such as the quasi-biennial oscillation  
128 (QBO) cycle and volcanic eruptions that perturb aerosol concentrations, etc., (ii) longer-term "external" effects  
129 such as the 11-year solar cycle, and (iii) longer-term internal trends in stratospheric ozone as a result of  
130 anthropogenic causes [Kivi *et al.*, 2007; Manney *et al.*, 2011]. A more comprehensive discussion of the annual  
131 cycle, inter-annual variability and also day-to-day variability of stratospheric ozone over Sodankylä may be  
132 found in Kivi *et al.* [2007].

133

### 134 **3.2 Variations of Stratospheric Ozone with Solar and Geophysical Parameters**

135

136 The literature contains various modelling and case-study results that show links between the state of the  
137 incoming solar wind, the subsequent state of the magnetosphere, and the terrestrial ozone population, in  
138 particular ozone in the mesosphere and ozone in the stratosphere. Considering the stratosphere, two physical  
139 mechanisms have been suggested that are thought to cause changes in the ozone population based on solar-wind  
140 driving; (i) instantaneous destruction of O<sub>3</sub> due to EPP by extremely energetic incident protons (with energies  
141 greater than ~100 MeV), whereby these penetrate the atmosphere directly to near-stratospheric altitudes and  
142 cause immediate ozone dissociation, and (ii) a longer time-scale process whereby odd-nitrogen species, for  
143 example, are created at mesospheric altitudes (by lower-energy particle precipitation due to both electrons or  
144 protons) and these then descend to stratospheric altitudes during the polar winter. At stratospheric altitudes  
145 these species cause chemical destruction of ozone. The latter process is often termed in the indirect effect, and  
146 the former the direct effect. Initially, we aim to test the efficacy of the direct effect by exploring links between  
147 solar-wind/geophysical parameters with the stratospheric ozone partial pressure. To investigate near-  
148 instantaneous changes in the ozone population we aim to correlate between the measured ozone partial pressure  
149 and the level of various geophysical parameters measured 24 hours previously.

150

151 Figure 3 contains plots of the ozonesonde observations as a function of altitude, and four geophysical and solar-  
152 wind parameters, namely: (i) The Auroral Electrojet (AE) index, a commonly used parameter that is a good  
153 proxy for magnetospheric substorm activity [Davis and Sugiura, 1966; Gjerloev et al., 2004], (ii) the solar-wind  
154 electric field parameter ( $-v_{sw}B_z$ ) calculated as the negative product of the solar-wind velocity ( $v_{sw}$ ) and the z-  
155 component of the solar-wind magnetic field ( $B_z$ ), and measured in units of  $\text{mV m}^{-1}$ , (iii) the adjusted F10.7  
156 index, a measure of the incident radio flux at 10.7 cm, and a good proxy for ionising solar EUV radiation  
157 [Tapping, 2013, and references therein], and (iv) the Disturbance Storm Time (Dst) index [Sugiura, 1964;  
158 Sckopke, 1966], a widely used measure of magnetospheric storm strength and a proxy for the strength of the  
159 Earth's ring current, measured in units of nT. All parameters used are taken from the hourly OMNI2 database  
160 [King and Papitashvili, 2005]. The aim of this analysis is to search for trends showing near-instantaneous  
161 changes in the ozone population as a result of changes driven by external solar wind parameters. If present,  
162 such changes could then be linked to direct destruction of stratospheric ozone by energetic particle precipitation.  
163

164 It is clear from the plots shown in Figure 3 that there is little evidence for such changes on a systematic basis.  
165 None of the plots show clear trends in the ozone partial pressure as a result of increases or decreases in the  
166 parameters examined. Perhaps the most surprising result here is that there is no clear correlation with the F10.7  
167 index since stratospheric ozone is known to be correlated with solar irradiance [Kivi et al., 2008]. In Figure 1  
168 the highest ozone levels (above the mean) come in years around solar maximum although this isn't by any  
169 means a hard and fast rule. For example, in 2006 near solar minimum, the average ozone levels were above  
170 average even though the F10.7 index during the year rarely exceeded 100. It is known that other physical  
171 variables also strongly affect the annual transport and destruction of stratospheric ozone during each year and  
172 that these can certainly suppress variations based on the UV variation alone (see for example Kivi et al. [2007]  
173 and Manney et al. 2011]).

174  
175 Whilst the literature does contain example case-studies of some of the largest geomagnetic storms resulting in  
176 rapid decreases in stratospheric ozone, it is also known that many of these 'extreme' events contain multiple  
177 drivers of geomagnetic activity such that no single index currently accounts for all causes of driving. The  
178 results from Figure 3 provide evidence that using fluctuations in a single geophysical index alone are not  
179 sufficient to use as a predictor of subsequent changes in the near-instantaneous ozone partial pressure in the  
180 stratosphere. If such changes are occurring, a more sophisticated analysis to reveal them is required.

181

### 182 3.3 The Effects of Solar-Proton Events (SPEs) on Stratospheric Ozone

183

184 In order to explore changes in stratospheric ozone, beyond the systematic seasonal variations shown in Figure 1,  
185 and the annual variations shown in Figure 2, we examine external driving of the atmosphere by solar-proton  
186 events. Many studies of non-terrestrial drivers of changes in the ozone population focus on such events, since  
187 the particle spectrum is sufficiently hard that the most energetic particles can penetrate deep into the  
188 mesosphere, into the stratosphere, and even to ground level (e.g. *Solomon et al.* [1981], *Thomas et al.* [1983],  
189 *Jackman and McPeters.* [1985], *Clilverd et al.* [2005], *Verronen et al.* [2011] *Damiani et al.* [2016], *Hocke*  
190 [2017]). For the most energetic solar-terrestrial event yet known in the modern era, the 1859 Carrington Event,  
191 it has even proved possible to model the effects of extremely high fluxes of solar protons on the ozone balance  
192 within the atmosphere [*Rodger et al.*, 2008]. However, in contrast to event studies of very large events, or  
193 theoretical studies of long-term trends, it has proven difficult to make estimates of the long-term effects of more  
194 frequent, but less extreme, events particularly on a regional level. A recent study by *Damiani et al.* [2016] has  
195 addressed this issue, in part, for the southern hemisphere by showing a 10-15% decrease in stratospheric ozone  
196 over Antarctica using limb-sounding methods from the Aura satellite. That study found that descent of  
197 mesospheric NO<sub>x</sub> down to stratospheric heights was the primary cause of such stratospheric ozone depletion in  
198 the southern hemisphere. The authors also highlighted the limited observational evidence available to quantify  
199 particle precipitation effects upon the ozone budget in general [*Damiani et al.*, 2016]. Here, we attempt to  
200 address this issue for the northern hemisphere.

201

202 As a basis for the analysis we utilize a list of 191 Solar Proton Events taken from the published list by the US  
203 National Oceanic and Atmospheric Administration (NOAA) Space Weather Prediction Center (SWPC) and  
204 freely available via file transfer protocol (<ftp://ftp.swpc.noaa.gov/pub/indices/SPE.txt>). At the time of the  
205 analysis, only one SPE event was listed beyond the end of 2015. The epoch times taken from the NOAA list are  
206 the start-times of each individual SPE, at a time resolution of one-hour.

207

208 Analysis is then carried out by performing a superposed epoch study of the measured ozone during these events.  
209 All available ozonesonde data are binned as a function of epoch time (time from SPE-onset) and geopotential  
210 altitude. The final grid for this binning is one day in time and 1 km in geopotential altitude, and spans a total of

211 90 days: 30 days prior to the SPE through to 60 days after the SPE. In addition, a set of 2500 randomly selected  
212 epochs between 1989 and 2015 are generated using the methodology of *Park and Miller* [1988]. The ozone data  
213 are then sorted based on these random epochs with this analysis providing a control data set against which the  
214 SPE analysis can be compared. Note that no account is made of short-term diurnal effects.

215

216 Figure 4 contains a selection of plots resulting from this analysis and shows the ozone partial pressure as a  
217 function of geopotential altitude and epoch time for (a) 2500 random epochs selected between 1989 and 2015  
218 (left column), and (b) 191 solar proton events that occurred during the same interval (right column). The plots  
219 show the averaged (mean) ozone partial pressure up to 40 km altitude (top row). No adjustment is made for  
220 seasonal variations in the data at this point. Also shown are line plots of the integral of the ozone partial  
221 pressure for altitudes between 16 and 24 km (middle row) for these events. This altitude region contains the  
222 bulk of stratospheric ozone (cf. Figure 1). The red points represent the individual data (i.e. the mean ozone  
223 partial pressure) and the blue line is a 15-day running box-car average of these data. (Note: the reduction in the  
224 running mean commences slightly prior to zero-epoch due to the 15-day averaging, although the individual (red)  
225 data points indicate ozone remains high until SPE arrival). The grey shading indicates the standard deviation of  
226 the superposition, whilst the thin orange, black, and purple lines represent the upper quartile, the median, and  
227 the lower quartile of the superposition.

228

229 The plots in the top two rows of Figure 4, although suggestive of a decrease in total stratospheric ozone  
230 following SPE occurrence, take no account of the large seasonal variations in the ozone partial pressure known  
231 to exist over Sodankylä. In order to remove the seasonal variations in the data contributing to the superposed  
232 epoch analysis the mean ozone partial pressure for the month in question (taken from the values in Figure 1) is  
233 subtracted from each data point. The resulting quantity is thus seasonally independent. The bottom row in  
234 Figure 4 shows the summation of these 'difference-from-mean' values. Here, a negative value indicates a  
235 seasonally independent (i.e. a true) reduction in ozone partial pressure. As can be seen from Figure 4, there are  
236 only small fluctuations in the ozone partial pressure in all three plots for the random epochs. However, for the  
237 SPEs there is clear evidence for a decrease in the ozone partial pressure that commences close to the zero epoch  
238 and reaches a minimum value after around 8 days. This is evident especially in the line plots showing the  
239 summed ozone partial pressure. Here, the decrease in the ozone partial pressure (summed between 16-24 km) is  
240 of the order of 5%. The seasonally adjusted ozone partial pressure immediately prior to the zero epoch is

241 slightly above the mean value but then falls rapidly around zero epoch, reaching a minimum after around 8 days,  
242 and then remains below the seasonally adjusted mean value for around 40 days.

243

244 While it is unlikely that protons with energies lower than ~10-100 MeV will directly reach the atmosphere  
245 above Sodankylä due to geomagnetic field rigidity effects (see *Rodger et al.* [2008], Figure 8), these protons  
246 will produce NO<sub>x</sub> at higher latitudes. This is then likely to be rapidly mixed throughout the polar vortex, and  
247 thus may contribute to indirect, time-delayed ozone depletion, particularly when the polar vortex extends to the  
248 Sodankylä region. This occurs around 50% of the time between December and April and never between July  
249 and October [*Kivi et al.*, 2007 - Table 3]. In order to test for such seasonal trends in the ozone observations we  
250 further sub-divide the data shown in Figure 4 based upon day of year.

251

252 Figure 5 shows the same series of plots as shown in Figure 4, but this time the data are only shown for the  
253 months July, August, September, and October (JASO) - periods when the polar vortex is absent over northern  
254 Finland [*Kivi et al.*, 2007]. In comparison with Figure 4, it is clear that changes in ozone following SPEs during  
255 these months are practically absent. There are fluctuations around the mean level throughout the epoch period,  
256 but there is little evidence for any systematic decrease in ozone partial pressure during these SPEs.

257

258 Figure 6 shows the same series of plots as shown in Figure 4 and Figure 5, but here the data are only shown for  
259 the months January, February, March, and April (JFMA); periods when the polar vortex is frequently present  
260 over northern Finland (~50% of the time) and can cause more rapid descent of long-lived NO<sub>x</sub> during hours of  
261 darkness. In contrast with the plots in Figure 4 and Figure 5, it is clear that a large reduction in the stratospheric  
262 ozone partial pressure occurs immediately following SPE arrival at Earth. This reduction persists for many  
263 days. Again, the reduction in the running mean commences slightly prior to zero-epoch in the 15-day running  
264 average, although the individual (red) data points do not show evidence of a decrease until zero epoch. We also  
265 note that prior to zero-epoch the ozone for the SPE events is already greater than the mean value - this is due to  
266 the fact that the SPEs are more common during the years around solar maximum, when ozone levels tend to be  
267 slightly elevated. In general, years around solar maximum have higher ozone concentrations on average,  
268 although this trend clearly isn't true in all years. It is strongly depends on other factors that affect the production  
269 and the loss of ozone (e.g. catalytic loss of ozone in the springtime caused by ClO and BrO reactions) [cf.  
270 *Manney et al.*, 2011].

271

272 Clearly, the reduction in ozone commencing at zero epoch is significant, being of the order of 10% during  
273 JFMA when the polar vortex is active over northern Finland. A minimum decrease is reached ~8 days on  
274 average after the SPE and ozone remains at a level below the mean value for ~40 days, and continues to  
275 fluctuate beyond this time. This result supports the interpretation that destruction of stratospheric ozone is  
276 occurring, due to the external driver of solar-wind proton precipitation. While the reduction in measured  
277 stratospheric ozone following SPE-arrival is clearly evident in Figure 6, the descent of NO<sub>x</sub> in the polar vortex  
278 at these lower altitudes is quite slow: around 8 km/month at ~50 km altitude [Manney *et al.*, 1994; Rinsland *et*  
279 *al.*, 2005]. Hence, a more-gradual response in the observed ozone decrease might be expected, rather than a  
280 decrease immediately following SPE arrival at Earth. A delay in the destruction of ozone, due to NO<sub>x</sub>  
281 production via electron precipitation, is also possible (e.g. Andersson *et al.* [2014], Randall *et al.* [2015]).  
282 Further studies are required to pin down the ultimate causes of the ozone depletion revealed here, and such  
283 studies are underway. Based on the literature, it is anticipated that these causes likely will include an admixture  
284 of direct and indirect physical mechanisms.

285

### 286 **3.4 Stratospheric Ozone Changes During High-speed Solar-wind Streams (HSSs)**

287

288 Stimulus for the work carried out in this manuscript originally arose from the knowledge that high-speed solar-  
289 wind streams (HSSs) are associated with enhanced activity in the Earth's magnetosphere and subsequently with  
290 large increases in energetic particle precipitation originating from the plasma sheet and/or radiation belts, noted  
291 by a number of authors (e.g. Sandanger *et al.*, [2007], Longden *et al.* [2008], Rodger *et al.* [2008], Denton *et al.*  
292 [2009], Borovsky and Denton [2009], Morley *et al.* [2012], Kavanagh *et al.* [2012], Hendry *et al.* [2013],  
293 Clilverd *et al.* [2013], Blum *et al.* [2015]). Although the energy spectrum during HSS-events is much softer  
294 than during SPEs there is still ongoing energetic particle precipitation, primarily due to relativistic (>1 MeV)  
295 electrons. Given the long-lived nature of HSSs such precipitation persists for much longer time intervals  
296 whether as continuous low-energy precipitation [Whittaker *et al.*, 2014;] or in the form of electron microbursts  
297 [Nakamura *et al.*, 2000; Lorentzen *et al.*, 2001; Blum *et al.*, 2015]. Indeed, ozone decreases in the middle  
298 atmosphere have been clearly observed during medium energy precipitation [Andersson *et al.*, 2014]. Using the  
299 data set described above, a search for substantial changes in stratospheric ozone partial pressure in the days  
300 following HSS-arrival, including times when the polar vortex was active, was carried out. The results from that

301 study proved inconclusive (figure not shown).

302

#### 303 **4. Discussion and Conclusions**

304

305 The analysis and results shown above highlight the difficulty in extracting changes in stratospheric ozone due to  
306 a single variable. However, by removing the monthly mean variations from the measured ozone partial  
307 pressure, and by concentrating on intervals when the polar vortex is active, and hence can assist in the descent of  
308 NO<sub>x</sub> species, it has been clearly demonstrated that solar protons are causing substantial stratospheric ozone  
309 depletion of the order of 10%, following SPEs.

310

311 Determination of ozone variability on the Earth's climate is of great topical interest although reviews of the  
312 behaviour of ozone throughout the atmosphere have tended to concentrate on internal terrestrial variables  
313 [Staelin *et al.*, 2001], or long-term solar changes [Haigh, 2003] rather than directly on short-term solar-  
314 induced forcing via SPEs. We argue that external driving of the Earth's stratospheric ozone budget was  
315 somewhat under-appreciated originally with studies initially concentrating on effects in the upper stratosphere  
316 and mesosphere [Rusch *et al.*, 1981; Solomon *et al.*, 1981; 1983]. Changes in the lower stratosphere due to  
317 external driving are now receiving more attention in the literature. Where solar-proton effects on climate are  
318 considered within global climate models, the effects have been reported as not statistically significant with  
319 regard to the annually averaged temperature and the total ozone variation (e.g. Jackman *et al.* [2009]).  
320 Although incorporation of the effects of short-term solar-proton fluctuations in global coupled climate models  
321 is currently quite rare, the effects of solar protons have been included in other modelling studies previously  
322 (e.g. Jackman and McPeters [1985]; Jackman *et al.* [1996]; Rodger *et al.* [2008]). SPEs have also been shown  
323 to produce local changes to stratospheric ozone on a case-by-case basis (e.g. Weeks *et al.* [1972]; Heath *et al.*  
324 [1977]; Thomas *et al.* [1983]; López-Puertas *et al.* [2005]; Seppälä *et al.* [2006]; Seppälä *et al.* [2008]).  
325 However, since most energy is deposited above 40 km, the direct effects of SPEs in general have not been  
326 considered important for quantification of total global ozone losses (e.g. Sinnhuber *et al.* [2003]), despite the  
327 long-lived nature of NO<sub>x</sub> species generated at higher altitudes allowing their descent to occur over a period of  
328 weeks or months (e.g. Randall *et al.* [2001]). The full effects of SPEs may not be appreciated by study of  
329 single events. In this study, superposed epoch analysis of 191 SPEs has enabled a longer-duration statistical  
330 investigation of the average changes in ozone partial pressures to be carried out. Our work emphasises the need

331 to incorporate energetic particle precipitation into climate models and we acknowledge the recent efforts in this  
332 direction (e.g. *Matthes et al.* [2017]).

333

## 334 **5. Summary**

335

336 In summary, we have analyzed data from 1845 balloon ozonesondes launched from Sodankylä, northern  
337 Finland, between 1989 and 2015. The mean monthly variation of stratospheric ozone has been calculated. The  
338 data have been analysed with respect to a number of geophysical variables (the AE index, the F10.7 index, the  
339 solar wind electric field parameter, and the Dst index), although no direct correlations to between stratospheric  
340 ozone and these indices (with a 24 hour time lag) was found.

341

342 To the best of our knowledge, this is the first comprehensive statistical study using balloon ozonesonde data that  
343 has provided direct, and long-term, in-situ evidence for stratospheric ozone depletion by SPEs in the northern  
344 hemisphere.

345

346 The results from this study are:

347

348 1. The average stratospheric ozone measured over northern Finland is highly variable during the year. The  
349 mean of the ozone partial pressure is greatest in winter and early spring and minimised in summer and early  
350 autumn.

351

352 2. There is no clear evidence for direct correlations between the stratospheric ozone partial pressure and the AE  
353 index, the F10.7 index, the solar-wind electric field, or the Dst index measured on the previous day.

354

355 3. A superposed epoch analysis of 191 SPEs examined between 1989 and 2015 indicates a fall in the ozone  
356 partial pressure of ~5% with a minimum reached ~8 days (on average) after the SPE arrival. The ozone partial  
357 pressure remains reduced below its mean value for ~40 days.

358

359 4. When only time intervals are considered when the polar vortex is present over northern Finland (i.e. late  
360 winter) the fall in ozone partial pressure is ~10% with the minimum again reached after ~8 days (on average)

361 after SPE arrival. The ozone remains reduced below its mean value for ~40 days. In contrast, no decrease in  
362 ozone is found following SPEs that occur during the northern hemisphere summer months of July-October when  
363 the polar vortex is not present.

364

365 It is intended that this study will highlight the fact that the average stratospheric ozone reduction is significant  
366 (~10%) following SPEs during the northern polar winter. We also intend that this knowledge be utilised to  
367 separate anthropogenic causes of ozone loss from natural causes. As noted in Section 2, balloon ozonesonde  
368 data have the advantage over satellite data that they provide high spatial resolution altitude profiles of the ozone  
369 distribution throughout the lower stratosphere. We plan on future analysis of other measured ozone data sources  
370 to investigate if the above findings are truly global or local (i.e. polar latitudes only) in nature. A follow-up  
371 study, using the same methodology but utilizing global satellite data coupled with multi-station balloon  
372 ozonesonde data from inside and outside the polar vortex, would certainly address this issue. In an era when  
373 separating anthropogenic ozone depletion from natural ozone depletion is receiving widespread attention, the  
374 results from this current study, summarised above, are particularly timely in that they provide quantification of  
375 the expected average ozone reduction for a number of events rather than quantifying such losses during single-  
376 event case-studies. Such averaged results should prove simpler to include in global climate models.

377

## 378 **Acknowledgements**

379 This work was supported at the Space Science Institute by the NASA Heliophysics LWS program via grants  
380 NNX14AN90G and NNX16AB75G, the NASA Heliophysics GI program via grant NNX14AC15G, and the  
381 NSF GEM program award number 1502947. Ozonesonde work at the FMI was supported by the Academy of  
382 Finland (grant number 140408); an EU Project GAIA-CLIM; the ESA's Climate Change Initiative programme  
383 and the Ozone\_cci subproject in particular. The work was originally conceived under the EU LAPBIAT II  
384 project (contract RITA-CT-2006-025969) and the authors gratefully acknowledge this support. MHD would  
385 like to thank Andrew Senior and Joe Borovsky for helpful comments and suggestions regarding data analysis,  
386 and the magnetospheric consequences of SPEs and HSSs, respectively. MHD offers particular thanks to all at  
387 Sodankylä Geophysical Observatory and the Finnish Meteorological Institute for their gracious hospitality  
388 during his visits to Sodankylä in the spring of 2008, 2012, and 2017.

389

## 390 **References**

391

392 Andersson, M., P. T. Verronen, C. J. Rodger, M. A. Clilverd, and A. Seppälä, Missing driver in the Sun–Earth  
393 connection from energetic electron precipitation impacts mesospheric ozone, *Nature Comm.*, 5,  
394 doi:10.1038/ncomms6197, 2014.

395

396 Blum, L., X. Li, and M. Denton, Rapid MeV electron precipitation as observed by SAMPEX/HILT during high-  
397 speed stream-driven storms, *J. Geophys. Res. Space Physics*, 120, 3783–3794, 2015.

398

399 Borovsky, J. E., and M. H. Denton, Relativistic-electron dropouts and recovery: A superposed epoch study of  
400 the magnetosphere and the solar wind, *J. Geophys. Res.*, 114, A02201, doi:10.1029/2008JA013128, 2009.

401

402 Butchart, N., The Brewer-Dobson circulation, *Rev. Geophys.*, 52, doi:10.1002/2013RG000448, 2014.

403

404 Clilverd, M. A., N. Cobbett, C. J. Rodger, J. B. Brundell, M. H. Denton, D. P. Hartley, J. V. Rodriguez, D.  
405 Danskin, T. Raita, and E. L. Spanswick, Energetic electron precipitation characteristics observed from  
406 Antarctica during a flux dropout event, *J. Geophys. Res. Space Physics*, 118, doi:10.1002/2013JA019067, 2013.

407

408 Clilverd, M. A., C. J. Rodger, T. Ulich, A. Seppälä, E. Turunen, A. Botman, and N. R. Thomson, Modelling a  
409 large solar proton event in the southern polar atmosphere, *J. Geophys. Res.*, 110, A09307,  
410 doi:10.1029/2004JA010922, 2005.

411

412 Crutzen, P. J., I. S. A. Isaksen, and G. C. Reid, Solar proton events: Stratospheric sources of nitric oxide,  
413 *Science*, 189, 457-458, 1975.

414

415 Damiani, A., M. Storini, M. Laurenza, and C. Rafanelli, Solar particle effects on minor components of the polar  
416 atmosphere, *Ann. Geophys.*, 26, 361–370, 2008.

417

418 Damiani, A., P. Diego, M. Laurenza, M. Storini and C. Rafanelli, Ozone variability related to several SEP  
419 events occurring during solar cycle no. 23, *Adv. Space Res.*, 43, 28-40, 2009.

420

421 Damiani, A., et al., Impact of January 2005 solar proton events on chlorine species, *Atmos. Chem. Phys.*, 12,  
422 4159–4179, 2012.

423

424 Damiani, A., B. Funke, M. L. Puertas, M. L. Santee, R. R. Codero, and S. Watanabe, Energetic particle  
425 precipitation: A major driver of the ozone budget in the Antarctic upper stratosphere, *Geophys. Res. Lett.*, 43,  
426 3554-3562, 2016.

427

428 Davis, T. N., and M. Sugiura, Auroral electrojet activity index AE and its universal time variations, *J. Geophys.*  
429 *Res.*, 71(3), 785–801, 1966.

430

431 Denton, M. H., J. E. Borovsky, M. Stepanova, and J. A. Valdivia, Preface: Unsolved Problems of  
432 Magnetospheric Physics, *J. Geophys. Res.*, 121, 10,783–10,785, 2016.

433

434 Denton, M. H., T. Ulich, and E. Turunen, Modification of midlatitude ionospheric parameters in the F2 layer by  
435 persistent high-speed solar wind streams, *Space Weather*, 7, S04006, 2009.

436

437 Deshler, T., R. Stübi, F. J. Schmidlin, J. L. Mercer, H. G. J. Smit, B. J. Johnson, R. Kivi, and B. Nardi, Methods  
438 to homogenize ECC ozonsonde measurements across changes in sensing solution concentration or ozonsonde  
439 manufacturer, *Atmos. Meas. Tech. Discuss.*, doi:10.5194/amt-2016-415 (under review), 2017.

440

441 Deshler, T., J. L. Mercer, H. G. J. Smit, R. Stubi, G. Levrat, B. J. Johnson, S. J. Oltmans, R. Kivi, A. M.  
442 Thomson, J. Witte, J. Davies, F. J. Schmidlin, G. Brothers, and T. Sasaki, Atmospheric comparison of  
443 electrochemical cell ozonesondes from different manufacturers, and with different cathode solution strengths:  
444 The Balloon Experiment on Standards for Ozonesondes, *J. Geophys. Res.*, 113, D04307,  
445 doi:10.1029/2007JD008975, 2008.

446

447 J. W. Gjerloev, R. A. Hoffman, M. M. Friel, L. A. Frank, J. B. Sigwarth. Substorm behavior of the auroral  
448 electrojet indices. *Annales Geophysicae*, European Geosciences Union, 2004, 22 (6), 2135-2149, 2004.

449

450 Haigh, J. D., The effects of solar variability on the Earth's climate, *Phil. Trans. R. Soc. Lond. A.*, 361, 95-111,

451 2003.

452

453 Heath, D. F., A. J. Kruger, and P. J. Crutzen, Solar proton events: Influence on stratospheric ozone, *Science*,

454 197, 886-889, 1977.

455

456

457 Hendry, A. T., C. J. Rodger, M. A. Clilverd, N. R. Thomson, S. K. Morley, T. Raita, Rapid radiation belt losses

458 occurring during high-speed solar wind stream-driven storms: Importance of energetic electron precipitation, in

459 *Dynamics of the Earth's Radiation Belts and Inner Magnetosphere*, Geophys. Monogr. Ser., vol. 199, edited by

460 D. Summers et al., 213–223, AGU, Washington, D. C., doi:10.1029/2012GM001299, 2013.

461

462 Hocke, K., Response of the middle atmosphere to the geomagnetic storm of November 2004, *J. Atmos. Sol-*

463 *Terr. Phys.*, 154, 86-91, 2017.

464

465 Jackman, C. H., and R. D. McPeters, the response of ozone to solar proton events during solar cycle 21: A

466 theoretical interpretation, *J. Geophys. Res.*, 90, 7955-7966, 1985.

467

468 Jackman, C. H., R. D. Marsh, F. M. Vitt, R. R. Garcia, C. E. Randall, E. L. Fleming, and S. M. Frith, Long-term

469 middle atmospheric influence of very large solar proton events, *J. Geophys. Res.*, 114, D11304,

470 doi:10.1029/2008JD011415, 2009.

471

472 Jackman, C. H., E. L. Fleming, S. Chandra, D. B. Considine, and J. E. Rosenfield, Past, present, and future

473 modeled ozone trends with comparisons to observed trends, *J. Geophys. Res.*, 101, 28753-28767, 1996.

474

475 Jackman, C. H., M. C. Cerniglia, J. E. Nielsen, D. J. Allen, J. M. Zawodny, R. D. McPeters, A. R. Douglass, J.

476 E. Rosenfield, and R. B. Hood, Two-dimensional and three-dimensional model simulations, measurements, and

477 interpretation of the October 1989 solar proton events on the middle atmosphere, *J. Geophys. Res.*, 100, 11641-

478 11660, 1995.

479

480 Kavanagh, A. J., F. Honary, E. F. Donovan, T. Ulich, and M. H. Denton, Key features of >30 keV electron

481 precipitation during high speed solar wind streams: A superposed epoch analysis, *J. Geophys. Res.*, 117,  
482 A00L09, 2012.

483

484 King, J. H., and N. E. Papitashvili, Solar wind spatial scales in and comparisons of hourly Wind and ACE  
485 plasma and magnetic field data. *J. Geophys. Res.*, 110, A02209, doi:10.1029/2004JA010804, 2005.

486

487 Kivi, R., E. Kyrö, T. Turunen, N. R. P. Harris, P. von der Gathen, M. Rex, S. B. Anderson, and I. Wohltmann,  
488 Ozonesonde observations in the Arctic during 1989-2003: Ozone variability and trends in the lower stratosphere  
489 and free troposphere, *J. Geophys. Res.*, 112, D08306, doi:10.1029/2006JD007271, 2007.

490

491 Kurt, V., A. Belov, H. Mavromichalaki, and M. Gerontidou, Statistical analysis of solar proton events, *Ann.*  
492 *Geophys.*, 22, 2255–2271, 2004.

493

494 Longden, N., M. H. Denton, and F. Honary, Particle precipitation during ICME-driven and CIR-driven  
495 geomagnetic storms, *J. Geophys. Res.*, 113, A06205, 2008.

496

497 Lopéz-Puertas, M., B. Funke, S. Gil-Lopéz, T. V. Clarmann, G. P. Stiller, M. Höpfner, S. Kellmann, H. Fischer,  
498 and C. H. Jackman, Observation of NO<sub>x</sub> enhancement and ozone depletion in the Northern and Southern  
499 hemispheres after the October-November 2003 solar proton events, *J. Geophys. Res.*, 110, A09S43,  
500 doi:10.1029/2005JA011050, 2005.

501

502 Lorentzen, K.R., Looper, M.D., Blake, J. B., Relativistic electron microbursts during the GEM storms,  
503 *Geophys. Res. Lett.*, 28, 2573, 2001.

504

505 Matthes, Funke, Andersson, Barnard, Beer, Charbonneau, Clilverd, Dudok de Wit, Haberreiter, Hendry,  
506 ackman, Kretzschmar, Kruschke, Kunze, Langematz, Marsh, Maycock, Misios, Rodger, Scaife, Seppälä,  
507 Shangguan, Sinnhuber, Tourpali, Usoskin, van de Kamp, Verronen, and Versick, Solar Forcing for CMIP6,  
508 Geoscientific Model Development, doi:10.5194/gmd-2016-9, (in oress), 2017.

509

510 Manney, G. L., Santee, M. L., Rex, M., Livesey, N. J., Pitts, M. C., Veefkind, P., Nash, E. R., Wohltmann, I.,

511 Lehmann, R., Froidevaux, L., Poole, L. R., Schoeberl, M. R., Haffner, D. P., Davies, J., Dorokhov, V.,  
512 Gernandt, H., Johnson, B., Kivi, R., Kyro, E., Larsen, N., Levelt, P. F., Makshtas, A., McElroy, C. T.,  
513 Nakajima, H., Parrondo, M. C., Tarasick, D. W., von der Gathen, P., Walker K. A., and Zinoviev, N. S.:  
514 Unprecedented Arctic Ozone loss in 2011, *Nature*, 478, 469–475, 2011.  
515  
516 Manney, G. L., R. W. Zurek, A. O'Neil, and R. Swinbank, On the motion of air through the stratospheric polar  
517 vortex, *J. Atmos. Sci.*, 51, 2973 – 2994, 1994.  
518  
519 Morley, S. K., R. H. W. Friedel, T. E. Cayton, and E. Noveroske, A rapid, global and prolonged electron  
520 radiation belt dropout observed with the Global Positioning System constellation, *Geophys. Res. Lett.*, 37,  
521 L06102, 2010.  
522  
523 Nakamura, R., Isowa, M., Kamide, Y., Baker, D.N., Blake, J.B., Looper, M., SAMPEX observations of  
524 precipitation bursts in the outer radiation belt, *J. Geophys. Res.*, 105, 15875, 2000.  
525  
526 Oh, S. Y., Y. Yi, J. W. Bieber, P. Evenson, and Y. K. Kim, Characteristics of solar proton events associated  
527 with ground level enhancements, *J. Geophys. Res.*, 115, A10107, 2010.  
528  
529 Park, S. K., and K. W. Miller, Random Number Generators: Good Ones are Hard to Find, *Communications of*  
530 *the ACM*, Vol. 31, No. 10, p. 1192-1201, 1988.  
531  
532 Randall, C. E., V. L. Harvey, L. A. Holt, D. R. Marsh, D. E. Kinnison, B. Funk and P. F. Bernath, Simulation of  
533 energetic particle precipitation effects during the 2003-2004 Arctic winter, *Journal of Geophysical Research :  
534 Space Physics*, 120, 5035–5048, doi:10.1002/2015JA021196, 2015.  
535  
536 Randall, C. E., D. E. Siskind, and R. M. Bevilaqua, Stratospheric NO<sub>x</sub> enhancements in the southern hemisphere  
537 vortex in winter/spring of 2000, *Geophys. Res. Lett.*, 28, 2385-2388, 2001.  
538  
539 Reames, D. V., Particle acceleration at the Sun and in the heliosphere, *Space Sci. Rev.*, 90, 413–491, 1999.  
540

541 Rinsland, C. P., C. Boone, R. Nassar, K. Walker, P. Bernath, J. C. McConnell, and L. Chiou, Atmospheric  
542 Chemistry Experiment (ACE) Arctic stratospheric measurements of NO<sub>x</sub> during February and March 2004:  
543 Impact of intense solar flares, *Geophys. Res. Lett.*, 32, L16S05, 2005.

544

545 Rodger, C. J., P. T. Verronen, M. A. Clilverd, A. Seppälä, and E. Turunen, Atmospheric impact of the  
546 Carrington event solar protons, *J. Geophys. Res.*, 113, D23302, doi:10.1029/2008JD010702, 2008.

547

548 Rodger, C. J., M. A. Clilverd, J. C. Green, and M. M. Lam, Use of POES SEM-2 observations to examine  
549 radiation belt dynamics and energetic electron precipitation into the atmosphere, *J. Geophys. Res.*, 115, A04202,  
550 2010.

551

552 Rodger, C. J., M. A. Clilverd, P. T. Verronen, Th. Ulich, M. J. Jarvis, and E. Turunen, Dynamic geomagnetic  
553 rigidity cutoff variations during a solar proton event, *J. Geophys. Res.*, 111, A04222,  
554 doi:10.1029/2005JA011395, 2006.

555

556 Rusch, D. W., J.-C. Gérard, S. Solomon, P. J. Crutzen, and G. C. Reid, The effect of particle precipitation events  
557 on the neutral and ion chemistry of the middle atmosphere: I. Odd nitrogen, *Planet. Space Sci.*, 29(7), 767, 1981.

558

559 Ryan, N. J., K. A. Walker, U. Raffalski, R. Kivi, J. Gross, and G. L. Manney, Ozone profiles above Kiruna  
560 from two ground-based radiometers, *Atmos. Meas. Tech.*, (under review), 2017.

561

562 Sandanger, M., F. Søråas, K. Aarsnes, K. Oksavik, and D. S. Evans, Loss of relativistic electrons: Evidence for  
563 pitch angle scattering by electromagnetic ion cyclotron waves excited by unstable ring current protons, *J.*  
564 *Geophys. Res.*, 112, A12213, doi:10.1029/2006JA012138, 2007.

565

566 Sckopke, N., A general relation between the energy of trapped particles and the disturbance field near the earth,  
567 *J. Geophys. Res.*, 71, 3125, 1966.

568

569 Seppälä, A., C. E. Randall, M. A. Clilverd, E. Rozanov, and C. J. Rodger, Geomagnetic activity and polar  
570 surface air temperature variability, *J. Geophys. Res.*, 114, A10312, doi:10.1029/2008JA014029, 2009.

571

572 Seppälä, A., M. A. Clilverd, C. J. Rodger, P. T. Verronen, and E. Turunen, The effects of hard-spectra solar  
573 proton events on the middle atmosphere, *J. Geophys. Res.*, 113, A11311, doi:10.1029/2008JA013517, 2008.

574

575 Seppälä, A., P. T. Verronen, V. F. Sofieva, J. Tamminen, E. Kyrölä, C. J. Rodger, and M. A. Clilverd,  
576 Destruction of the tertiary ozone maximum during a solar proton event, *Geophys. Res. Lett.*, 33, L07804,  
577 doi:10.1029/2005GL025571, 2006.

578

579 Seppälä, A., P. T. Verronen, E. Kyrölä, S. Hassinen, L. Backman, A. Hauchecorne, J. L. Bertaux, and D.  
580 Fussen, Solar proton events of October–November 2003: Ozone depletion in the Northern Hemisphere polar  
581 winter as seen by GOMOS/Envisat, *Geophys. Res. Lett.*, 31, L19107, 2004.

582

583 Sinnhuber, M., J. P. Burrows, M. P. Chipperfield, C. H. Jackman, M-B. Kallenrode, K. F. Künzi, and M. Quack,  
584 A model study of the impact of magnetic field structure on atmospheric composition during solar proton events,  
585 *Geophys. Res. Lett.*, 30, 15, 1818, doi:10.1029/2003GL017265, 2003.

586

587 Shumilov, O. I., E. A. Kasatkina, V. A. Turyansky, E. Kyrö, and R. Kivi, Solar cosmic ray effects in  
588 atmospheric chemistry evidenced from ground-based measurements, *Adv. Space Res.*, 31, 9, 2157-2162, 2003.

589

590 Smit, H. G. J. and the ASOPOS panel (Assessment of Standard Operating Procedures for Ozonesondes):  
591 Quality assurance and quality control for ozonesonde measurements in GAW, World Meteorological  
592 Organization, GAW Report #201, Geneva, Switzerland, 2014. available at:  
593 [http://www.wmo.int/pages/prog/arep/gaw/documents/FINAL\\_GAW\\_201\\_Oct\\_2014.pdf](http://www.wmo.int/pages/prog/arep/gaw/documents/FINAL_GAW_201_Oct_2014.pdf).

594

595 Solomon, S., D. W. Rusch, J. C. Gérard, G. C. Reid, and P. Crutzen, The effect of particle precipitation on the  
596 neutral and ion chemistry of the middle atmosphere: II odd hydrogen, *Planet. Space Sci.*, 29, 885-892, 1981.

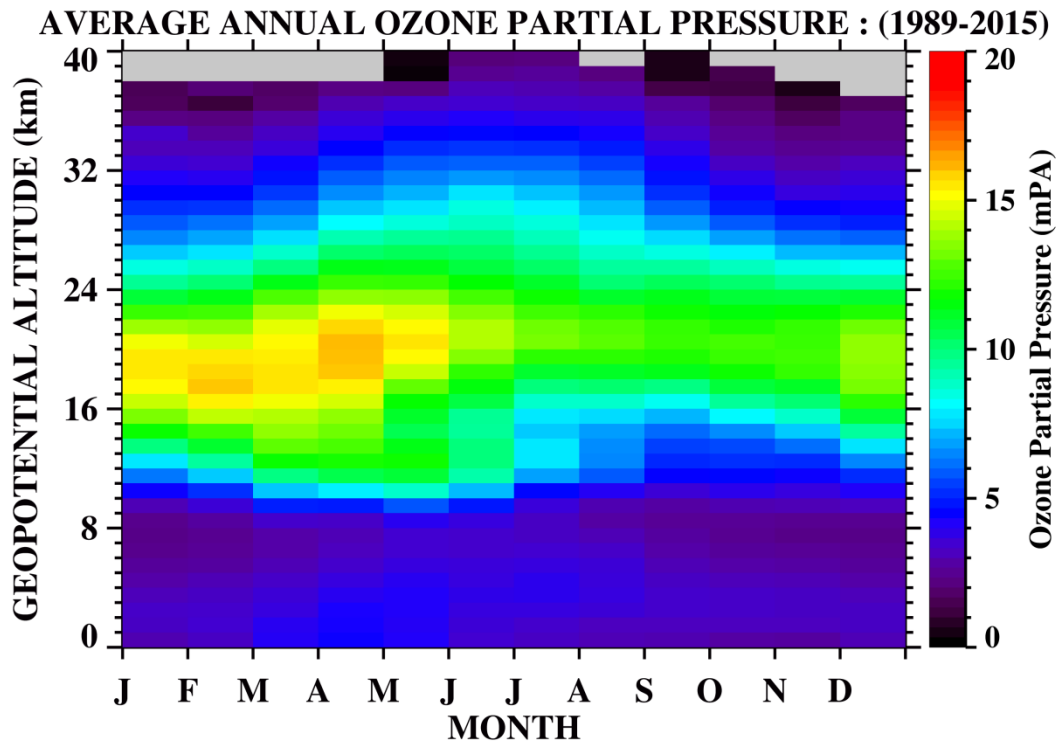
597

598 Solomon, S., D. W. Rusch, R. J. Thomas, and R. S. Eckman, Comparison of mesospheric ozone abundance  
599 measured by the Solar Mesosphere Explorer and model calculations, *Geophys. Res. Lett.*, 10, 249–252,  
600 doi:10.1029/GL010i004p00249, 1983.

601  
602 Staehelin, J., N. R. P. Harris, C. Appenzeller, and J. Eberhard, Ozone trends: A review, *Rev. Geophys.*, 39, 231-  
603 290, 2001.  
604  
605 Tapping, K. F., The 10.7 cm solar radio flux ( F 10.7 ), *Space Weather*, 11, 394–406, 2013.  
606  
607 Thomas, R. J., C. A. Barth, G. J. Rottman, D. W. Rusch, G. H. Mount, G. M. Lawrence, R. W. Sanders, G. E.  
608 Thomas, L. E. Clemens, Mesospheric ozone depletion during the solar proton event of July 13, 1982: Part 1  
609 Measurement, *Geophys. Res. Lett.*, 10, 253-255, 1983.  
610  
611 Turunen, E., A. Kero, P. T. Verronen, Y. Miyoshi, S.-I. Oyama, and S. Saito, Mesospheric ozone destruction by  
612 high-energy electron precipitation associated with pulsating aurora, *J. Geophys. Res. Atmos.*, 121,  
613 doi:10.1002/2016JD025015, 2016.  
614  
615 Tylka, A. J., C. M. S. Cohen, W. F. Dietrich, M. A. Lee, C. G. MacLennan, R. A. Mewaldt, C. K. Ng, and D. V.  
616 Reames, A comparative study of ion characteristics in the large gradual solar energetic particle events of 2002  
617 April 21 and 2002 August 24, *Astrophys. J. Suppl. Ser.*, 164, 536–551, 2006.  
618  
619 Verronen, P. T., and R. Lehmann, Analysis and parameterisation of ionic reactions affecting middle atmospheric  
620 HO<sub>x</sub> and NO<sub>y</sub> during solar proton events, *Ann. Geophys.*, 31, 909–956, doi:10.5194/angeo-31-909-2013, 2013.  
621  
622 Verronen, P. T., M. L. Santee, G. L. Manney, R. Lehmann, S.-M. Salmi, and A. Seppala, Nitric acid  
623 enhancements in the mesosphere during the January 2005 and December 2006 solar proton events, *J. Geophys.*  
624 *Res.*, 116, D17301, 2011.  
625  
626 Sugiura, M., Hourly values of equatorial Dst for the IGY, *Ann. Int. Geophys. Year*, 35, 9, Pergamon Press,  
627 Oxford, 1964.  
628  
629 Weeks, L. H., R. S. CuiKay, and J. R. Corbin, Ozone measurements in the mesosphere during the solar proton  
630 event of 2 November 1969, *J. Atmos. Sci.*, 29, 1138-1142, 1972.

631

632 Whittaker, I. C., M. A. Clilverd, and C. J. Rodger, Characteristics of precipitating energetic electron fluxes  
633 relative to the plasmopause, *J. Geophys. Res.*, 119, 8784–8800, doi:10.1002/2014JA020446, 2014.

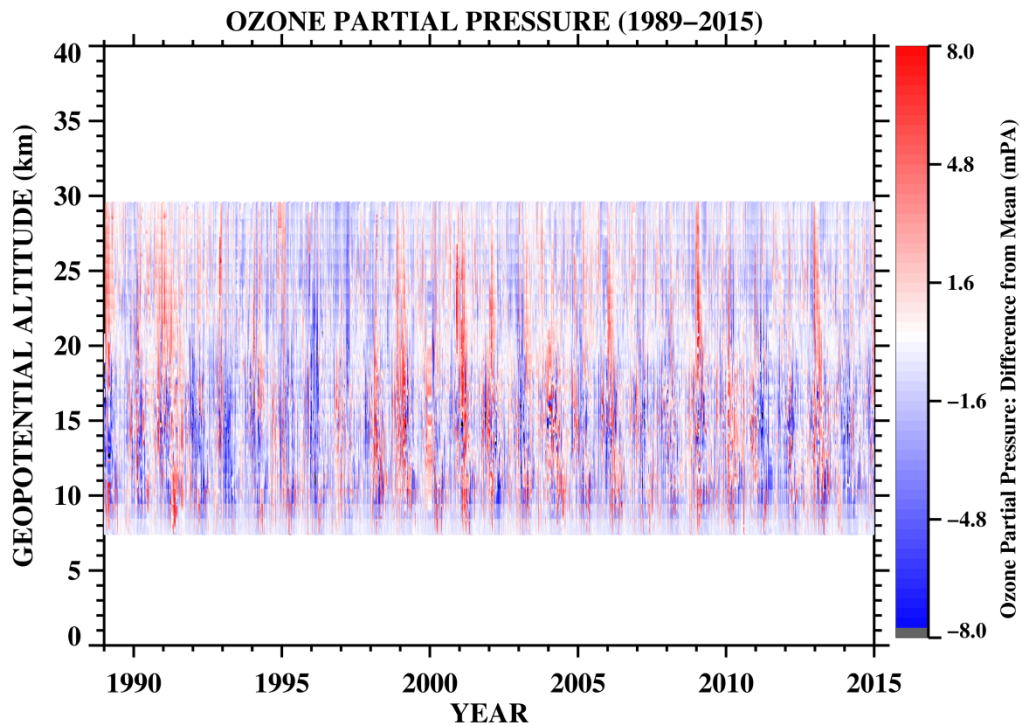
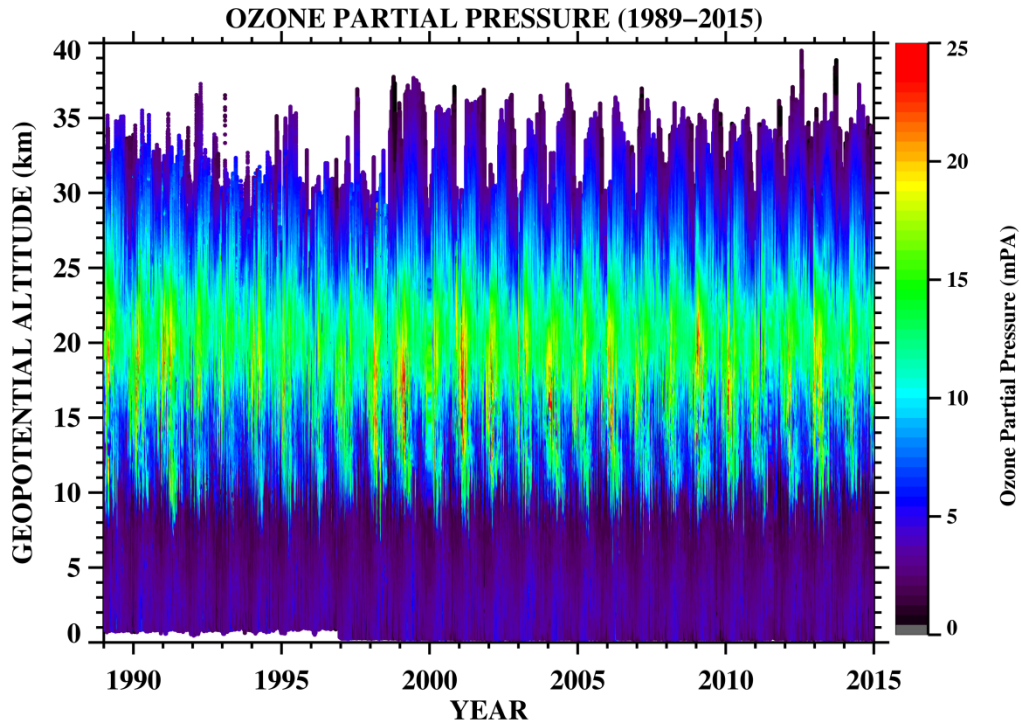


635

636

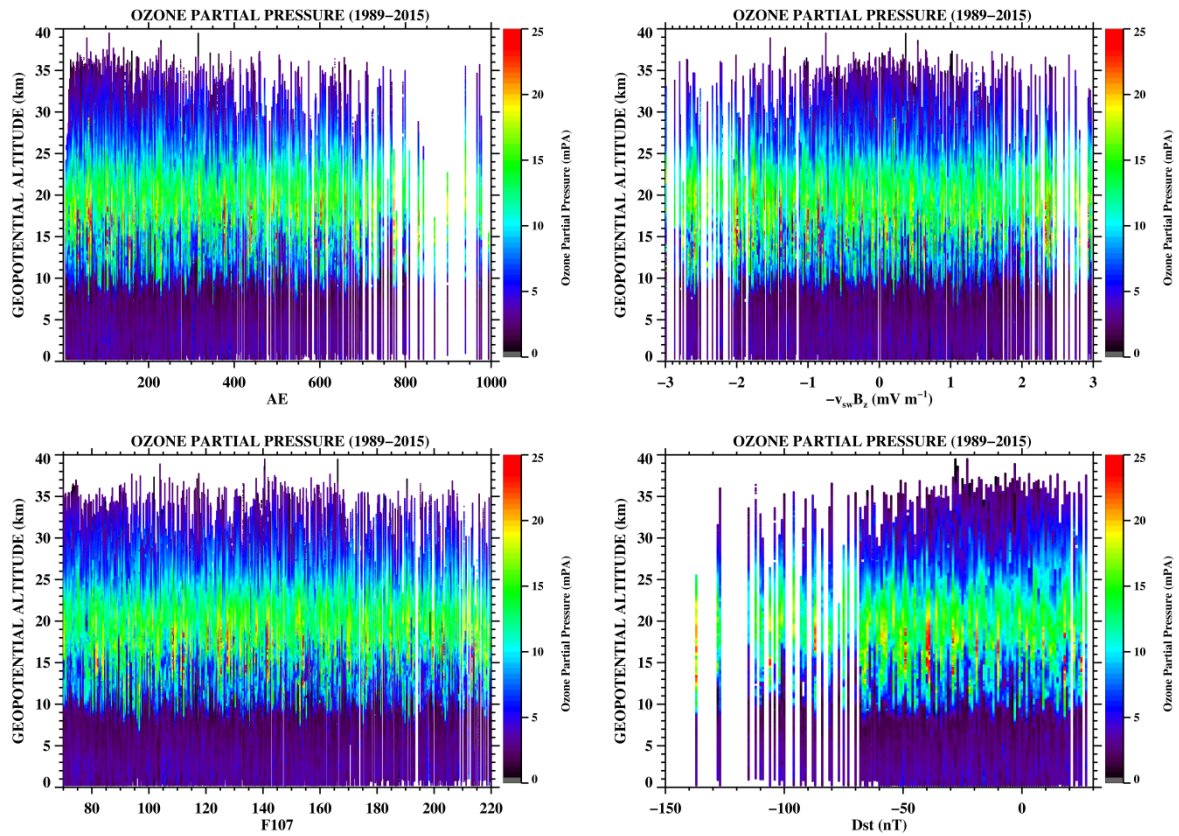
637 **FIGURE 1:** The averaged ozone partial pressure (in mPa) as a function of geopotential altitude and month-of-  
 638 the-year for 1845 balloon ozonesondes launched between 1989 and 2015 from Sodankylä, northern Finland.  
 639 Ozone is higher in winter/early-spring months and lower in summer/autumn months. (Note: This analysis  
 640 updates the previous analysis of *Kivi et al.* [2007], Figure 4).

641



643

644 **FIGURE 2:** Showing a time-series of all ozonesonde data from Sodankylä between 1989 and 2015. The top  
 645 plot shows the ozone partial pressure as a function of year and geopotential altitude. The bottom figure shows  
 646 the same data (8-30 km altitude only), but this time adjusted for the seasonal mean variations using the data  
 647 from Figure 1. Positive values (red) indicate measurements that are higher than the long-term mean and  
 648 negative (blue) values show measurements that are lower than the long-term mean.



649

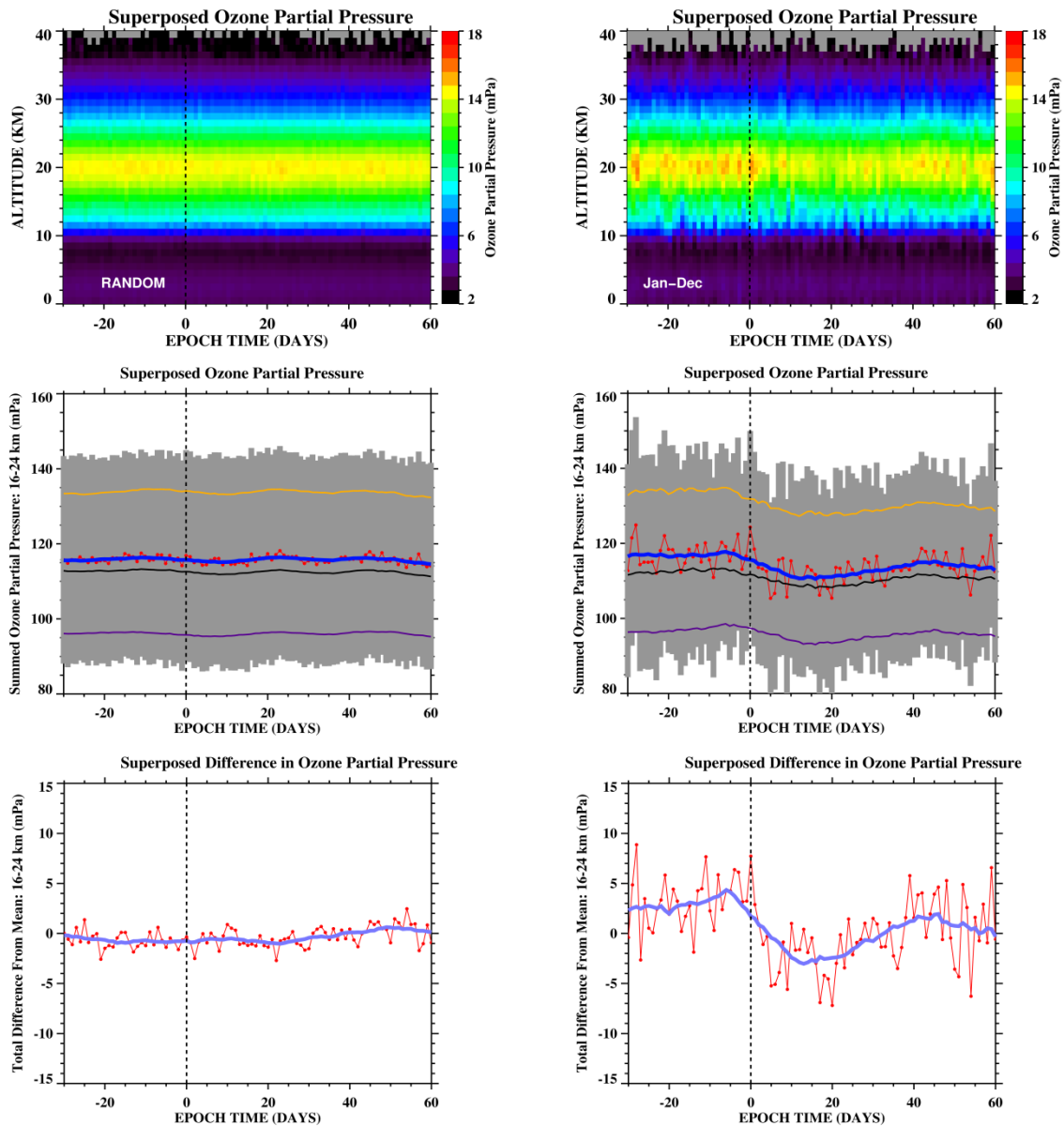
650

**FIGURE 3:** Plots showing the variation of the ozone partial pressure as a function of geopotential altitude in kilometres with (i) the AE index, (ii) the solar-wind electric field parameter  $-v_{sw}B_z$ , (iii) the F10.7 index, and (iv) the Dst index. There is little evidence for systematic changes in the ozone partial pressure with any of these four parameters.

652

653

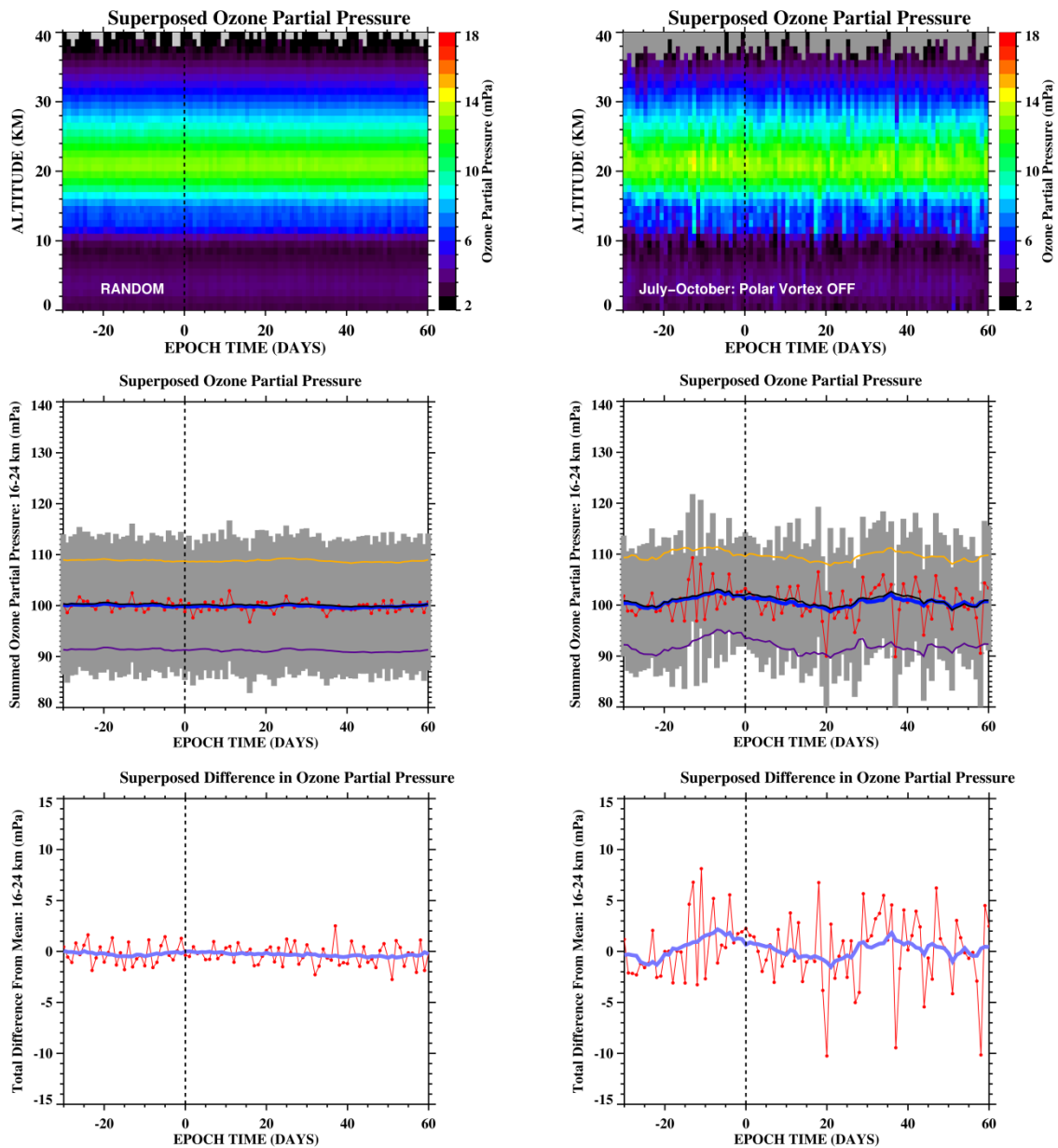
654



656

657 **FIGURE 4:** Showing the ozone partial pressure as a function of geopotential altitude and epoch time for (a)  
 658 2500 random epochs selected between 1989 and 2015 (left column), and (b) 191 solar proton events that  
 659 occurred during the same interval (right column). The plots show the averaged ozone partial pressure up to 40  
 660 km altitude (top row), the integral of the ozone partial pressure between 16 and 24 km altitude (middle row), and  
 661 the integrated difference-from-mean quantity, also between 16 and 24 km altitude (note: data become sparse in  
 662 for altitudes  $>>35$ km). The red points represent the individual data and the blue line is a 15-day running box-car  
 663 average for these data. The grey shading indicates the standard deviation of the superposition, whilst the thin  
 664 orange, black, and purple lines represent the upper quartile, the median, and the lower quartile of the  
 665 superpositions. There is a clear decrease in the ozone partial pressure following the arrival of solar proton  
 666 events.





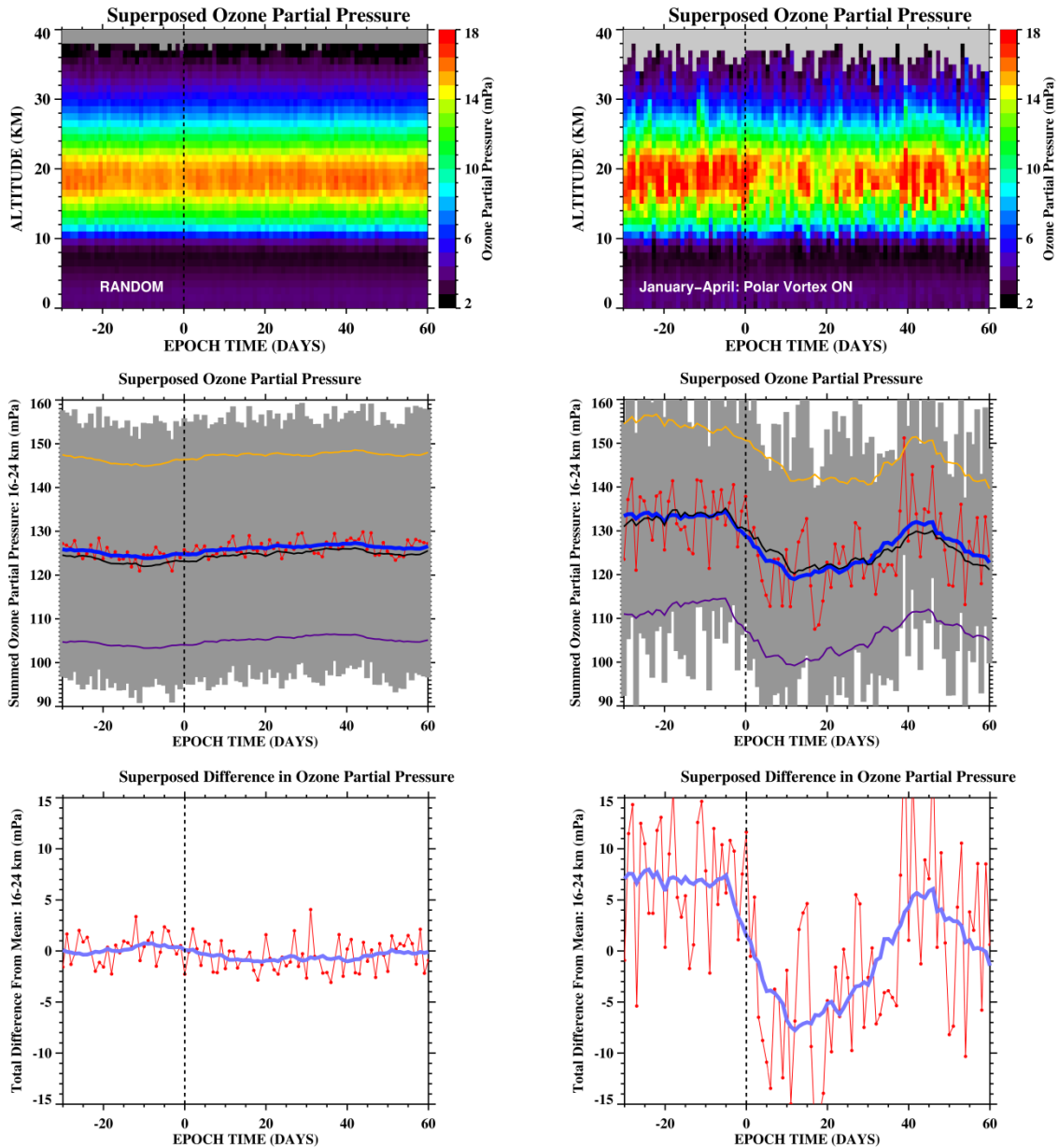
668

669

**FIGURE 5:** The same format as shown in Figure 4, but here data are only plotted for July, August, September, and October when the polar vortex is INACTIVE over Northern Finland. There is no clear trend for changes in the stratospheric ozone population following the SPEs.

671

672



674

675 **FIGURE 6:** The same format as shown in Figure 4 and Figure 5, but here data are only plotted for January,  
 676 February, March and April, when the polar vortex is ACTIVE over Northern Finland. There is a clear trend for  
 677 a decrease in the stratospheric ozone population following the SPEs.

678